LBL-37148
UC-603
Preprint

Lawrence Berkeley Laboratory
UNIVERSITY OF CALIFORNIA

EARTH SCIENCES DIVISION

Submitted to Water Resources Research

The Laplace Transform Finite Difference Method for the Solution of the Solute Transport Problem in Groundwater: 1. Theory

G.J. Moridis and D.L. Reddell

April 1995

REFERENCE COPY
Does Not
Circulate
Bldg. 50 Library.
LBL-37148
Copy 1

Prepared for the U.S. Department of Energy under Contract Number DE-AC03-76SF00098

DISCLAIMER

This document was prepared as an account of work sponsored by the United States Government. While this document is believed to contain correct information, neither the United States Government nor any agency thereof, nor the Regents of the University of California, nor any of their employees, makes any warranty, express or implied, or assumes any legal responsibility for the accuracy, completeness, or usefulness of any information, apparatus, product, or process disclosed, or represents that its use would not infringe privately owned rights. Reference herein to any specific commercial product, process, or service by its trade name, trademark, manufacturer, or otherwise, does not necessarily constitute or imply its endorsement, recommendation, or favoring by the United States Government or any agency thereof, or the Regents of the University of California. The views and opinions of authors expressed herein do not necessarily state or reflect those of the United States Government or any agency thereof or the Regents of the University of California.

LBL-37148
UC-603

The Laplace Transform Finite Difference Method for the Solution of the Solute Transport Problem in Groundwater: 1. Theory

G. J. Moridis
Earth Sciences Division
Lawrence Berkeley Laboratory
University of California
Berkeley, CA 94720

and

D. L. Reddell
Agricultural Engineering Department
Texas A&M University
College Station, TX 77843-2117

April 1995

This work was supported by the Texas Agricultural Experiment Station under grant 6993/91, and by the U.S. Department of Energy, Office of Environmental Management, Office of Technology Development, under Contract No. DE-AC03-76SF00098.

The Laplace Transform Finite Difference Method for the Solution of the Solute Transport Problem in Groundwater: 1. Theory

George J. Moridis
Earth Sciences Division, Lawrence Berkeley Laboratory
University of California, Berkeley

Donald L. Reddell
Department of Agricultural Engineering, Texas A&M University, College Station

Abstract. A new numerical method, the Laplace Transform Finite Difference (LTFD) method, is extended to the solution of the solute transport problem in groundwater. The major advantage of LTFD is that it eliminates the time dependency, the need for time discretization, and the problems stemming from the treatment of the time derivatives in the nonlinear Partial Differential Equations (PDEs) of flow and transport by using Laplace transform formulations. LTFD yields solutions semi-analytical in time and numerical in space by solving special formulations of the PDEs using a Finite Difference (FD) space discretization scheme in the Laplace space, and numerically inverting the transformed solution vectors. Two space discretization schemes are employed, and two inversion methods are used. Concerns over the effects of the numerical treatment of the time dependency on accuracy and stability, which necessitate a large number of small time steps between successive observation times in traditional solutions, are rendered irrelevant because time is no longer a consideration. An unlimited time step size is thus possible without loss of accuracy or stability.

1. Introduction

The contaminant transport problem in groundwater involves the solution of two Partial Differential Equations (PDEs): the parabolic PDE of groundwater flow, and the hyperbolic PDE of solute transport. The traditional numerical methods employed in the solution of these PDEs discretize both the space and the time domains, and are based on the universal concept of substitution of a set of algebraic equations (valid within subdomains of time and space) for the original equations. Instead of solving for a continuous smooth function $f(x_1, x_2, x_3, t)$, the space domain (x_1, x_2, x_3) is subdivided in M subdomains with spatially constant properties and the time t is discretized in M_t subdivions (timesteps); M_t sets of approximations $\tilde{f}$ of the solution are obtained at the M predetermined points in space. A PDE problem with a continuous smooth solution surface is thus reduced to a set of algebraic equations, which are easier to solve and provide a solution arithmetically "close" to the true solution of the original PDE, from which they differ by the truncation error $E = f - \tilde{f}$.

While the numerical solution of the PDE of transient groundwater flow is relatively simple, the solution of the hyperbolic PDE of solute transport in groundwater poses some formidable problems which may involve oscillating solutions, numerical dispersion, peak clipping, and grid orientation. For simultaneous flow and solute transport, the space discretization which minimizes truncation errors in the flow equation is rarely that which minimizes the truncation errors in the solute transport equation. This requires the development of complicated schemes (e.g. dual, adaptive, or travelling grids), which may be difficult to implement and require large computer storage memories.

Although space discretization may be very important (especially in cases of sharp fronts), the treatment of the time dependence and the approximation of the time derivative in the PDEs are consistently the most important factors affecting the stability and accuracy of the numerical methods approximating the PDE of solute transport. The

explicit formulation of the numerical approximation to the transport PDE may require impractically small time steps for stability. Implicit formulations may introduce significant numerical dispersion. Inappropriate time dicretization may lead to numerical smearing or oscillatory behavior of the solution, and especially so in cases of sharp fronts and dominant advective displacements. Unstable solutions, inaccurate results, and significant mass balance errors may be observed. Accuracy and stability considerations necessitate a large number of small timesteps between observation times, and solutions must be obtained at all these intermediate times (whether desired or not), at the expense of longer execution times and larger roundoff errors.

The Laplace Transform Finite Difference (LTFD) method is a numerical method developed for the solution of the linear parabolic PDE of incompressible flow [*Moridis and Reddell*,1990*a*; 1991*a*] and the non-linear PDE of slightly compressible fluid flow [*Moridis et al.*,1994] through porous media. It belongs to a family of new, Laplace-transform based numerical methods which also includes the Laplace Transform Galerkin [*Sudicky*,1989; 1990], the Laplace Transform Finite Element (LTFE) method [*Moridis and Reddell*,1991*b*], and the Laplace Transform Boundary Element (LTBE) method [*Moridis and Reddell*,1991*c*; 1992].

These methods combine traditional space discretization schemes with Laplace transforms, and use the same approach: (a) a Laplace transform is performed on the original PDE, (b) the resulting transformed PDE is discretized using a standard FD, FE, or BE discretization scheme, (c) the resulting simultaneous equations are solved and the vector of the unknowns is obtained in the Laplace space, and (d) the solution in real time is obtained by numerically inverting the Laplace space solution.

The major advantage of these new numerical methods is that they eliminate (a) the time dependency of the problem, (b) the complications arising from the treatment of the time derivative, and (c) thus the need for a large number of small timesteps for an

accurate solution because of their Laplace transform formulation. They return a solution numerical in space and semi-analytical in time, allow an unlimited timestep size without loss of accuracy or stability, and yield a stable, non-increasing material balance error in addition to a more accurate solution than the conventional treatments. Execution times may be reduced by orders of magnitude [*Moridis and Reddell*,1991*c*] because calculations are necessary only at the desired observation times, while in standard methods calculations are needed at all the intermediate times of the discretized time domain.

The combination of a traditional space discretization scheme with Laplace transforms for the solution of the solute transport equation was first reported by *Sudicky* [1989; 1990], who reported impressive results using a Galerkin weighted-residual variational formulation. Assuming (a) a constant, time-invariant velocity field, (b) a uniform porosity distribution, (c) linear absorption, and (d) a water density unaffected by the presence of solutes (i.e. very dilute solutions), he eliminated the flow equation from the problem and obtained numerical solutions of the linearized solute transport PDE in systems with Peclet numbers in excess of 30. For the numerical inversion of the solutions in the Laplace space he used the *Crump* [1976] algorithm (accelerated by means of the epsilon algorithm [*MacDonald*,1964]), which, though powerful, requires the solution of a large number of large, almost singular matrices (four times the size of the analogous matrix in the traditional time-marching Galerkin scheme), and significant execution times.

Expansion of LTFD for use in the solution of the hyperbolic solute transport PDE was first presented by *Moridis and Reddell* [1990*b*]. In this paper we present (a) the development of the generalized PDEs of transient flow and transport through porous media in an appropriate form for use in LTFD, (b) the LTFD formulation of both PDEs, (c) two space discretization schemes, as well as (d) two numerical schemes for the inversion of the solutions in the Laplace space. Applications of the methodology to a number of flow and transport problems are presented in a companion paper [*Moridis*,1995].

2. The Equation of Flow

2.1. General Form

The general non-linear equation of transient flow single-phase through porous media is obtained by combining appropriate forms of Darcy's Law and the equation of mass conservation, yielding:

$$\nabla \cdot \left[\frac{k\rho}{\mu} \cdot (\nabla P - \rho g \nabla h) \right] = \frac{\partial(\rho\phi)}{\partial t} + \tilde{q}, \tag{1}$$

where k is the absolute permeability tensor of the porous medium (L^2); ρ is the fluid density (ML^{-3}); μ is the fluid viscosity ($ML^{-1}T^{-1}$); P is the fluid pressure ($ML^{-1}T^{-2}$); g is the gravitational acceleration (LT^{-2}); h is the elevation (L); ϕ is the porous medium porosity (*dimensionless*); t is the time (T); and $\tilde{q}$ is the mass flow rate of source or sink per unit volume ($ML^{-3}T^{-1}$). If the effects of other factors (such as temperature) on the fluid density are negligible compared to the influence of pressure and concentration, the fluid density can be described by the expression

$$\begin{aligned} \rho(P, C) =& \rho_{00} \cdot (1 + \omega X) \cdot \exp\{\epsilon(P - P_0)\} = \\ & \rho_{0p} \cdot (1 + \omega X) = \rho_{c0} \cdot \exp\{\epsilon(P - P_0)\}, \end{aligned} \tag{2}$$

where

$$C = X \cdot C_0 \qquad \omega = \frac{C_0}{\rho_{0p}} \frac{\partial \rho}{\partial C} = \frac{1}{\rho_{0p}} \frac{\partial \rho}{\partial X}, \tag{3}$$

C is the contaminant mass concentration per unit volume of the fluid phase (ML^{-3}); X is the relative concentration (dimensionless), and $0 \leq X \leq 1$; C_0 is the reference concentration, usually equal to the maximum expected concentration (ML^{-3}); ϵ is the fluid compressibility ($M^{-1}LT^2$); P_0 is a reference pressure ($ML^{-1}T^{-2}$); ρ_{00} is the fluid density at $P = P_0$ and $C = 0$; ρ_{0p} is the density at $P = P$ and $C = 0$; and ρ_{c0} is the density at $P = P_0$ and $C = C$.

The viscosity μ is a weak function of concentration, and is given by

$$\mu = \mu_0(1 + \eta X), \quad \text{and} \quad \eta = \frac{C_0}{\mu_0} \frac{\partial \mu}{\partial C} = \frac{1}{\mu_0} \frac{\partial \mu}{\partial X}. \tag{4}$$

Viscosity is a weaker function of concentration than density, i.e. $\eta < \omega$.

The dependence of ϕ on pressure was described by *Moridis* [1987] as

$$\phi = 1 + (\phi_0 - 1)\ \exp\{(\xi + \zeta)(P_0 - P)\}\,, \tag{5}$$

where ϕ_0 is the porosity at $P = P_0$, ξ is the reservoir (aquifer) particle (grain) compressibility ($M^{-1}LT^2$), and ζ is the reservoir (aquifer) skeleton compressibility. From (2), (3) and (4)

$$\frac{\partial \rho}{\partial P} = \epsilon\ \rho_{c0}\ \exp\{\epsilon(P - P_0)\} = \epsilon\ \rho, \tag{6}$$

$$\frac{\partial \rho}{\partial X} = \omega\ \rho_{0p}, \tag{7}$$

and

$$\frac{\partial \phi}{\partial P} = (\phi_0 - 1)(\xi + \zeta)\ \exp\{(\xi + \zeta)(P_0 - P)\}\ . \tag{8}$$

2.2. Assumptions and Simplifications

In the development of the PDE of flow through porous media, isothermal flow and negligible lateral deformation of the aquifer skeleton were assumed. For groundwater flow, we can make the following simplifications with a negligible loss of accuracy:

1. The water viscosity is unaffected by pressure. This is a valid assumption because viscosity, while being strongly affected by temperature, is a very weak function of pressure for the range of pressures encountered in groundwater aquifers.

2. The pressure dependence of the density ρ in the flow terms (i.e. in the left-hand side) of (1) is neglected. This is a valid assumption for water ($\epsilon = 4.47 \times 10^{-10}\ 1/Pa$), where a pressure change equal to 220 times the atmospheric (very unusual under most near-surface groundwater conditions) is needed to effect an 1% change in ρ. Then

$$\rho_{0p} \simeq \rho_{00} \quad \text{and} \quad \rho \simeq \rho_{00}\ (1 + \omega X)\ . \tag{9}$$

3. Unless compressible clayey soils are involved, the values of ξ and ζ are very small ($\propto 10^{-11}$ - $10^{-9}\ 1/Pa$), and the following approximations can be made with negligible

effects on accuracy:

$$\phi = 1 + (\phi_0 - 1)\ \exp\{(\xi + \zeta)(P_0 - P)\} \simeq 1 + (\phi_0 - 1)\,[1 + (\xi + \zeta)(P_0 - P)] \simeq \phi_0\ , \quad (10)$$

and

$$\frac{\partial \phi}{\partial P} \simeq (1 - \phi_0)\ (\xi + \zeta)\ . \quad (11)$$

2.3. Development of the Right-Hand Side

Expanding the time derivative on the right-hand side of (1), we have

$$\begin{aligned} \frac{\partial(\rho\phi)}{\partial t} &= \left(\rho\frac{\partial \phi}{\partial P} + \phi\frac{\partial \rho}{\partial P}\right)\frac{\partial P}{\partial t} + \phi\frac{\partial \rho}{\partial X}\frac{\partial X}{\partial t} \\ &= \rho_{00}\ [\underbrace{S_p\ \frac{\partial P}{\partial t}}_{R1} + \underbrace{S_p\ \omega\ X\ \frac{\partial P}{\partial t}}_{R2} + \underbrace{S_c\ \frac{\partial X}{\partial t}}_{R3}\ ], \end{aligned} \quad (12)$$

where

$$S_p = (1 - \phi_0)\ (\xi + \zeta) + \phi_0\ \epsilon, \qquad S_c = \phi_0\ \omega, \quad (13)$$

and are constants.

Investigating the spatial and temporal behavior of $R1$, $R2$ and $R3$, we notice the following:

1. Due to the high speed of propagation of the pressure perturbation, flow achieves a steady-state in a relatively short time (i.e. a few hours or days) after the excitation of the system (caused by the operation of wells or a variation in the boundary conditions). On the other hand, the migration of solutes is a much slower process; while a local steady-state may be reached, a domain-wise steady-state may not be reached for hundreds or even thousands of days after the initial excitation of the system, and it may not be reached at all over the simulated period of the process.

2. For relatively short times t (i.e. before the time t_p when the pressure steady-state is reached) $R2$ is generally non-linear and $\frac{\partial P}{\partial t} \neq 0$, although it may tend to zero in areas not

yet affected by the excitation. Due to the small value of ω ($\leq 10^{-2}$), $R2$ can be linearized as

$$R2 \simeq \left(S_p\, \omega\, \overline{X}\right) \frac{\partial P}{\partial t}, \tag{14}$$

where $\overline{\chi}$ indicates the time averaged value of the quantity χ, i.e.

$$\overline{\chi} = \frac{1}{t} \int_0^t \chi \, dt. \tag{15}$$

This is especially true in cases of injection of solutes in previously 'clean' aquifers (i.e. $X = 0$), where (a) the extent of contaminant migration is limited in the time t_p needed to reach a pressure steady-state condition, (b) $R2$ is linear (and $R3 = 0$) both spatially and temporally over large sections of the domain (due to $X = 0$) during this time, and (c) the linearization in (14) is very accurate and conserves mass in the vicinity of the injection point.

3. In aquifers which are not bounded exclusively by no-flow boundaries, $\frac{\partial P}{\partial t} \rightarrow 0$ throughout the space domain after the initial short time t_p to the pressure steady-state condition. For $t \geq t_p$, $P(x_1, x_2, x_3, t) = P(x_1, x_2, x_3)$, the quantity $R2(x_1, x_2, x_3, t) \rightarrow 0$, and its non-linearity vanishes.

4. The quantities S_p and S_c being constants, $R1$ and $R3$ are linear. Due to the length of the time t_c required to reach the concentration steady-state, in general $R3 \neq 0$ during the duration of the simulation, though it is possible to have subdomains where $R2 = 0$.

2.4. Development of the Left-Hand Side

Substitution into and expansion of the left hand side of (1) yields

$$\frac{\partial}{\partial x_i} \left\{ \frac{k \rho_{00}}{\mu_0} \frac{(1+\omega X)}{(1+\eta X)} \left[\frac{\partial P}{\partial x_i} - \rho_{00}(1+\omega X) g h_i' \right] \right\}$$

$$= \underbrace{\frac{\rho_{00}}{\mu_0} \frac{\partial}{\partial x_i} \left[k \frac{(1+\omega X)}{(1+\eta X)} \frac{\partial P}{\partial x_i} \right]}_{L1} - \underbrace{\frac{\rho_{00}^2 g}{\mu_0} \frac{\partial}{\partial x_i} \left[k h_i' \frac{(1+\omega X)^2}{(1+\eta X)} \right]}_{L2}, \tag{16}$$

where $i \equiv 1,2,3$ and $h_i' = \frac{\partial h}{\partial x_i}$. Both $L1$ and $L2$ are non-linear. Expansion of $L1$ yields

$$L1 = \underbrace{\frac{\rho_{00}\omega}{\mu_0\eta}\,\frac{\partial}{\partial x_i}\left(k\frac{\partial P}{\partial x_i}\right)}_{L1a} - \underbrace{\frac{\rho_{00}(\omega-\eta)}{\mu_0\eta}\,\frac{\partial}{\partial x_i}\left(\frac{k}{1+\eta X}\,\frac{\partial P}{\partial x_i}\right)}_{L1b}.$$

The term $L1a$ is linear. In $L1b$, the term $(1+\eta X) \rightarrow 1$ when either $\eta \rightarrow 0$ (i.e. when the viscosity is unaffected by the concentration of a certain species) or $X \rightarrow 0$. An excellent approximation is obtained when $(1+\eta X)$ is linearized by using $(1+\eta\overline{X})$.

In $L2$ the quantity

$$\frac{(1+\omega X)^2}{(1+\eta X)} = 1 + \frac{\omega^2}{\eta}X + \frac{\beta}{(1+\eta X)}X, \quad \text{where} \quad \beta = 2\omega - \eta - \frac{\omega^2}{\eta} \tag{17}$$

is linearized by substituting $\overline{X}$ for X in the denominator of the third term of the sum. Introduction into $L2$, substitution and expansion leads to

$$L2 = \underbrace{\frac{\rho_{00}^2 g}{\mu_0}\,\frac{\partial}{\partial x_i}\left(kh_i{}'\right)}_{L2a} + \underbrace{\frac{\rho_{00}^2\omega^2 g}{\mu_0\eta}\,\frac{\partial}{\partial x_i}\left(kh_i{}'X\right)}_{L2b} + \underbrace{\frac{\rho_{00}^2\,\beta g}{\mu_0}\,\frac{\partial}{\partial x_i}\left(\frac{kh_i'}{1+\eta\overline{X}}\,X\right)}_{L2c}. \tag{18}$$

The term $L2a = L2a(x_1, x_2, x_3)$ is time-invariant. The term $L2b$ is linear, and may become significant in the long-term solute migration in deep aquifers.

Substitution into (1), division by ρ_{00}, and rearrangement yields

$$\begin{aligned}\frac{\partial}{\partial x_i}\left(K_{1P}\,\frac{\partial P}{\partial x_i}\right) + \frac{\partial}{\partial x_i}\left(K_{1X}\,X\right) - \frac{\rho_{00}g}{\mu_0}\,\frac{\partial}{\partial x_i}\left(kh_i'\right) \\ = S_t\,\frac{\partial P}{\partial t} + S_c\,\frac{\partial X}{\partial t} + q\,(1+\omega X_q),\end{aligned} \tag{19}$$

where

$$K_{1P} = \frac{k}{\mu_0}\left(\frac{\omega}{\eta} - \frac{\omega-\eta}{\eta(1+\eta\overline{X})}\right), \tag{20}$$

$$K_{1X} = -\frac{\rho_{00}g}{\mu_0}\left(\frac{\omega^2}{\eta} + \frac{\beta}{1+\eta\overline{X}}\right)kh_i{}', \tag{21}$$

$$S_t = S_p\,(1+\omega\overline{X}) \qquad \text{and} \qquad q = \tilde{q}/\rho_{00}. \tag{22}$$

q is the volumetric flow rate of a source or sink per unit volume (T^{-1}), and X_q is the relative concentration of the solute in the removed or injected water. Equation (19) describes the flow of almost incompressible fluids through porous media in its general form, with a minimum of simplifications. Although the formulation of (19) suggests cartesian coordinates, the equation of flow in cylindrical coordinates can be obtained in an entirely analogous manner through a procedure described in detail by *Moridis and Reddell* [1991*a*]. When low solute concentrations do not affect the water density, equation (19) applies with the adjustments

$$K_{1P} \simeq \frac{k}{\mu_0}, \quad K_{1X} \simeq -\frac{\rho_{00} g}{\mu_0}(2\omega - \eta)\, k h_i', \quad \text{and} \quad S_t \simeq S_p. \tag{23}$$

3. The Equations of Solute Transport

3.1. The Equation of a Species in Solution

The equation of transport of reacting solutes through porous media was presented in various forms by several investigators [*Bear*, 1972; *Domenico and Palciauskas*, 1979; *Hyakorn and Pinder*, 1983]. Applying the principles of mass conservation, the general non-linear transport equation of a single species is

$$\frac{\partial}{\partial x_i}\left(C_0 \mathbf{D}_{ij} \frac{\partial X}{\partial x_j}\right) - \frac{\partial}{\partial x_i}(C_0 V_i X) = \frac{\partial}{\partial t}(\phi C_0 X) + q C_0 X_q + A + \phi\Gamma \tag{24}$$

where $\mathbf{D}_{ij}$ is the tensor of hydrodynamic dispersion (L^2T^{-1}); V_i is the Darcy velocity (LT^{-1}) of the aqueous phase; A is the rate of mass transfer of the species between the liquid (solute) and the soil matrix (adsorbate) ($ML^{-3}T^{-1}$); and Γ is the rate of mass production/disappearance of the solute by homogeneous reaction per unit volume of liquid ($ML^{-3}T^{-1}$). $\mathbf{D}_{ij}$ includes both mechanical dispersion [*Scheidegger*,1961] and molecular diffusion [*Millington*,1959], and is given by *Dorgarten and Tsang* [1991] as

$$\mathbf{D}_{ij} = \delta_{ij}\alpha_t |V| + (\alpha_\ell - \alpha_t)\frac{V_i V_j}{|V|} + \delta_{ij}\phi^{4/3} D_m, \tag{25}$$

where δ_{ij} is the Kronecker delta, α_ℓ and α_t are the longitudinal and transverse dispersivities (L) respectively, and D_m is the molecular diffusivity (L^2T^{-1}).

Assuming linear reversible, non-equilibrium sorption, a general expression for A is [*Voss*,1984]

$$A = C_0(1-\phi)\ H, \qquad H = m_1 X + m_2 X_s, \tag{26}$$

where m_1 and m_2 are sorption parameters (T^{-1}), and X_s is the relative concentration of adsorbate on the grains of the porous medium (with respect to C_0). If a linear equilibrium sorption model is assumed, then

$$X_s = K_d X, \qquad \text{and} \qquad A = C_0(1-\phi)\ H, \qquad H = K_d\ \frac{\partial X}{\partial t}, \tag{27}$$

where K_d is a 'distribution coefficient'.

The production/disappearance term Γ is given by an expression of the type [*Voss*,1984]

$$\Gamma = C_0(\gamma_0 + \gamma_1 X), \tag{28}$$

where γ_0 and γ_1 are appropriate coefficients (such as decay coefficients in the case of radioactive decay). Equation (28) can be used to describe first-order production or decay such as radioactive decay, biological oxygen demand, and biological or chemical production, as well as zero-order production or decay.

Substituting in (24), and dividing by C_0, results in

$$\underbrace{\frac{\partial}{\partial x_i}\left(\mathbf{D}_{ij}\ \frac{\partial X}{\partial x_j}\right)}_{T1} - \underbrace{\frac{\partial}{\partial x_i}\ (V_i\ X)}_{T2} = \underbrace{\frac{\partial}{\partial t}\ (\phi X)}_{T3} + qX_q + (1-\phi)H + \phi(\gamma_0 + \gamma_1 C). \tag{29}$$

The terms $T1$, $T2$, and $T3$ are non-linear, but can be linearized with a minimal effect on accuracy using the procedures previously described. Investigation of the temporal behavior of V_i shows that after the relatively short period t_p, V_i becomes time-invariant, and equal to its steady-state value. We have found that in the absence of flow reversals, the approximation

$$\mathbf{D}_{ij} \simeq \overline{\mathbf{D}}_{ij} = \delta_{ij}\alpha_t\overline{|V|} + (\alpha_\ell - \alpha_t)\frac{\overline{V_i}\ \overline{V_j}}{\overline{|V|}} + \delta_{ij}\phi^{4/3}D_m, \tag{30}$$

allows the linearization of $T1$ with a minimal effect on accuracy for $t \leq t_p$ and no perceptible effect for $t > t_p$. Then

$$T1 \simeq \frac{\partial}{\partial x_i}\left(\overline{\mathbf{D}}_{ij}\,\frac{\partial C}{\partial x_j}\right). \tag{31}$$

The linearization of $T2$ follows the same logic and procedure, and yields

$$T2 = \frac{\partial}{\partial x_i}(V_i X) \simeq \frac{\partial}{\partial x_i}(\overline{V_i} X). \tag{32}$$

Similarly, expanding $T3$ and using (10),

$$T3 = (1-\phi_0)(\xi+\zeta)X\,\frac{\partial P}{\partial t} + \phi\,\frac{\partial X}{\partial t} \simeq (1-\phi_0)(\xi+\zeta)\overline{X}\,\frac{\partial P}{\partial t} + \phi_0\,\frac{\partial X}{\partial t}. \tag{33}$$

For ξ, $\zeta \rightarrow 0$ (incompressible formations), and $t > t_d$ (when $\frac{\partial P}{\partial t} \rightarrow 0$),

$$T3 \rightarrow \phi_0 \frac{\partial X}{\partial t}. \tag{34}$$

Substitution into (29) yields the linearized form of the equation of the species in solution in its most general form as

$$\begin{aligned} &\frac{\partial}{\partial x_i}\left(\overline{\mathbf{D}}_{ij}\,\frac{\partial X}{\partial x_j}\right) - \frac{\partial}{\partial x_i}(\overline{V_i} X) \\ &\quad = (1-\phi_0)(\xi+\zeta)\overline{X}\,\frac{\partial P}{\partial t} + \phi_0 \frac{\partial X}{\partial t} + qX_q + (1-\phi_0)H + \phi_0(\gamma_0 + \gamma_1 X). \end{aligned} \tag{35}$$

3.2. The Equation of the Adsorbate

The conservation of mass for a single species stored as adsorbate on the solid grains of a porous medium is expressed as

$$A - (1-\phi)\Gamma_s = \frac{\partial}{\partial t}\left[(1-\phi)C_0 X_s\right], \tag{36}$$

where A is given by equations (26) or (27). Γ_s is the rate of adsorbate mass production (per unit volume of the solid matrix) due to production/decay reactions within the adsorbed material, and

$$\Gamma_s = C_0(\gamma_{0s} + \gamma_{1s} X_s), \tag{37}$$

where γ_{0s} and γ_{1s} are appropriate coefficients (such as decay coefficients in the case of radioactive decay). Substituting into (36), expanding, linearizing, and dividing by C_0 yields

$$(1-\phi_0)H-(1-\phi_0)(\gamma_{0s}+\gamma_{1s}X_s)=-(1-\phi_0)(\xi+\zeta)\overline{X}_s\,\frac{\partial P}{\partial t}-\phi_0\,\frac{\partial X_s}{\partial t}. \tag{38}$$

3.3. The Final Form of the Equations

Equations (19), (35), and (38) govern the flow and solute transport in groundwater systems, subject to the previously discussed assumptions. If adsorption is not included, then equations (19) and (35) are solved simultaneously, with $H = 0$ in (35). For deep aquifers, long times, dense solutions, and reversible non-equilibrium adsorption, (19), (35), and (38) are solved simultaneously to yield P, X, and X_s.

If a linear equilibrium model is assumed, then $X_s = K_dX$, equation (38) of the adsorbate can be eliminated by adding it to equation (35), yielding

$$\begin{aligned}\frac{\partial}{\partial x_i}\left(\overline{\mathbf{D}}_{ij}\,\frac{\partial X}{\partial x_j}\right)-\frac{\partial}{\partial x_i}(\overline{V}_iX)\\ =\phi(1-K_d)\frac{\partial X}{\partial t}+\overline{X}(1-K_d)(1-\phi_0)(\xi+\zeta)\frac{\partial P}{\partial t}\\ +qX_q+\phi(\gamma_0+\gamma_1X)+(1-\phi)(\gamma_{0s}+\gamma_{1s}K_dX).\end{aligned} \tag{39}$$

Then equations (19) and (39) are solved simultaneously.

When low solute concentrations do not affect the liquid density, equation (19) is the equation of flow after the simplifications of equation (23). If the pore deformation is negligible, equation (39) is further simplified to

$$\begin{aligned}\frac{\partial}{\partial x_i}\left(\overline{\mathbf{D}}_{ij}\,\frac{\partial X}{\partial x_j}\right)-\frac{\partial}{\partial x_i}(\overline{V}_iX)\\ =\phi(1-K_d)\frac{\partial X}{\partial t}+qX_q+\phi(\gamma_0+\gamma_1X)+(1-\phi)(\gamma_{0s}+\gamma_{1s}K_dX).\end{aligned} \tag{40}$$

Then equations (19) and (40) are solved sequentially.

4. Step 1 of the Method: The Laplace Transform of the PDEs

The Laplace Transform Finite Difference (LTFD) numerical method eliminates the time dependency, the need for time discretization, and the problems stemming from the treatment of the time derivatives in the PDEs of flow and transport by providing a numerical solution in the Laplace space. This approach renders time step size considerations and limitations irrelevant, and allows an unlimited time step size without loss of accuracy or stability. The unknowns in time are obtained by numerically inverting the Laplace-space solution. The application of LTFD is described in detail in the following sections.

The Laplace transform of the PDEs of flow and transport is possible because of the linearization of the equations described in the previous sections. Applying the Laplace transform to the flow equation (19),

$$f_P(\Phi, \Psi, \Upsilon) = \frac{\partial}{\partial x_i}\left(K_{1P}\,\frac{\partial \Phi}{\partial x_i}\right) + \frac{\partial}{\partial x_i}\left(K_{1X}\;\Psi\right) + K_{2P}\;\Phi + K_{2X}\;\Psi = B_P, \tag{41}$$

where

$$K_{2P} = -S_t\;\lambda, \qquad K_{2X} = -S_c\;\lambda, \tag{42}$$

$$B_P = Q - S_t\;P_i\;-\;S_c\;X_i\;+\;\frac{g\rho_{00}}{\mu_0\lambda}\;\frac{\partial}{\partial x_i}\left(kh_i'\right), \tag{43}$$

P_i and X_i are the initial pressure and relative concentration, λ is the Laplace variable,

$$\Phi = \mathcal{L}\{P\}, \quad \Psi = \mathcal{L}\{X\}, \quad \text{and} \quad Q = \mathcal{L}\{q\;(1 + \omega X_q)\}, \tag{44}$$

and $\mathcal{L}\{\}$ denotes the Laplace transform of the quantity in the brackets. For injection at a steady rate q of water with a relative concentration X_q, $Q = q\;(1 + \omega X_q)/\lambda$. For water removal at a rate q, $Q = q/\lambda + q\omega\Psi$, and the terms K_{2X} and B_P are adjusted.

Application of the same procedures to equations (35) and (38) yields

$$f_X(\Phi, \Psi, \Upsilon) = \frac{\partial}{\partial x_i}\left(F_{1X}\;\frac{\partial \Psi}{\partial x_j}\right) - \frac{\partial}{\partial x_i}(F_{2X}\;\Psi) + F_{3X}\;\Psi + F_{1P}\;\Phi + F_{1S}\;\Upsilon = B_X \tag{45}$$

and

$$G_{1P}\;\Phi + G_{1X}\;\Psi + G_{1S}\;\Upsilon = B_S \tag{46}$$

respectively, where

$$F_{1X} = \overline{\mathbf{D}}_{ij}, \qquad F_{2X} = \overline{V_i}, \qquad F_{3X} = -\left[\phi_0(\lambda + \gamma_1) + (1 - \phi_0)\ m_1\right], \tag{47}$$

$$F_{1P} = -\overline{X}(1 - \phi_0)(\xi + \zeta)\ \lambda, \qquad F_{1S} = -(1 - \phi)\ m_2, \tag{48}$$

$$B_X = Q_c - \overline{X}(1 - \phi_0)(\xi + \zeta)\ P_i - \phi_0\ C_i + \frac{\phi_0\gamma_0}{\lambda}, \tag{49}$$

$$G_{1P} = -\overline{X_s}(1 - \phi_0)(\xi + \zeta)\ \lambda, \tag{50}$$

$$G_{1X} = (1 - \phi)\ m_2 + \phi_0\ \lambda, \quad G_{1S} = -(1 - \phi_0)\ (m_2 - \gamma_{1s}), \tag{51}$$

$$B_S = -\overline{X_s}(1 - \phi_0)(\xi + \zeta)\ P_i + \phi_0\ C_i + (1 - \phi_0)\ \gamma_{0s}\ \lambda, \tag{52}$$

$$\Upsilon = \mathcal{L}\{X_s\}, \quad \text{and} \quad Q_c = \mathcal{L}\{qX_q)\} = \begin{cases} qX_q/\lambda & \text{for injection,} \\ q\Psi & \text{for removal.} \end{cases} \tag{53}$$

For water removal the terms F_{3X} and B_X have to be adjusted. Equation (45) is the general equation of a species in solution. For solute transport with linear equilibrium adsorption, the Laplace transform of equation (39) yields an equation of the same form, but with

$$F_{3X} = -\left\{\phi_0\left[(1 - K_d)\lambda + \gamma_1\right] + (1 - \phi_0)\ K_d\ \gamma_{1s}\right\}, \tag{54}$$

$$F_{1P} = -\overline{X}(1 - K_d)(1 - \phi_0)(\xi + \zeta)\ \lambda, \qquad F_{1S} = 0, \tag{55}$$

and

$$\begin{aligned} B_X = Q_c &- \overline{X}(1 - K_d)(1 - \phi_0)(\xi + \zeta)\ P_i \\ &- \phi\ (1 - K_d)\ X_i + \frac{1}{\lambda}\left[\phi\gamma_0 + (1 - \phi_0)\ \gamma_{0s}\right]. \end{aligned} \tag{56}$$

For the dilute solutions described by equation (40), the general form of equation (45) is maintained with $F_{1S} = 0$, F_{3X} as in equation (54), but with

$$F_{1P} = 0 \quad \text{and} \quad B_2 = Q_c - \phi_0\ (1 - K_d)\ X_i + \frac{1}{\lambda}\left[\phi_0\gamma_0 + (1 - \phi_0)\ \gamma_{0s}\right]. \tag{57}$$

The criteria for the selection of the appropriate equations were discussed in subsection 3.3.

5. Step 2: The FD Scheme in the Laplace Space

Time being no longer considered, a standard "block centered" grid method is employed in the space discretization of the transformed PDEs of flow and transport [*Aziz and Settari*,1979]. There are M_1, M_2 and M_3 subdivisions of the x_1, x_2 and x_3 coordinates respectively, which divide the domain into $M = M_1 \times M_2 \times M_3$ gridblocks.

5.1. Approximation of Derivatives in the Flow Equation

In the LTFD method the spatial domain discretization is the same as in a standard FD scheme. The discretization of the term $\frac{\partial}{\partial x_i}(K_{1P}\ \frac{\partial \Phi}{\partial x_i})$ in the general equation of flow (41) follows the procedure discussed in detail by *Moridis and Reddell* [1991*a*].

5.2. Diffusion-Related Derivatives in the Transport Equation

The discretization of $\frac{\partial}{\partial x_i} \cdot (\phi_0 \overline{\mathbf{D}}_{ij}\ \frac{\partial \Theta}{\partial x_j})$ in the general transport equation (47) follows the procedures discussed by [*Reddell and Sunada*,1970]. Using the terms and quantities depicted in Figure 1, in a two-dimensional cartesian system $(x_1 \equiv x, x_2 \equiv y)$

$$\frac{\partial}{\partial x}\left(D_{xx}\ \frac{\partial \Psi}{\partial x}\right) \simeq \underbrace{\frac{(D_{xx})_{i+\frac{1}{2}}}{\Delta \ell_{x+}}}_{G_x^+}\ (\Psi_{i+1} - \Psi_i) + \underbrace{\frac{(D_{xx})_{i-\frac{1}{2}}}{\Delta \ell_{x-}}}_{G_x^-}\ (\Psi_{i-1} - \Psi_i)\,, \tag{58}$$

where $D_{xx} \equiv \overline{\mathbf{D}}_{11}$ for simplicity, and

$$\Delta \ell_{x\pm} = \frac{1}{2}\ \Delta x_i\ (\Delta x_{i\pm 1} + \Delta x_i). \tag{59}$$

The subscripts j and k are invariant in (58), and are omitted. The cross derivative

$$\frac{\partial}{\partial x}\left(D_{xy}\ \frac{\partial \Psi}{\partial y}\right) \simeq \frac{\left(D_{xy}\ \frac{\partial \Psi}{\partial y}\right)_{i+\frac{1}{2}} - \left(D_{xy}\ \frac{\partial \Psi}{\partial y}\right)_{i-\frac{1}{2}}}{\Delta x_i}$$

$$
\begin{aligned}
&= \overbrace{\frac{(D_{xy})_{i+\frac{1}{2}}}{\Delta \ell_{xy}}}^{G^+_{xy}} \left(a_{1i}\ \Psi_{i,j+1} + a_{2i}\ \Psi_{i+1,j+1} - a_{1i}\ \Psi_{i,j-1} - a_{2i}\ \Psi_{i+1,j-1}\right) \\
&- \underbrace{\frac{(D_{xy})_{i-\frac{1}{2}}}{\Delta \ell_{xy}}}_{G^-_{xy}} \left(b_{1i}\ \Psi_{i-1,j+1} + b_{2i}\ \Psi_{i,j+1} - b_{1i}\ \Psi_{i-1,j-1} - b_{2i}\ \Psi_{i,j-1}\right),
\end{aligned}
\tag{60}
$$

where

$$
a_{1i},\ b_{2i} = \frac{\Delta x_{i\pm 1}}{\Delta x_{i\pm 1} + \Delta x_i}, \qquad a_{2i},\ b_{1i} = \frac{\Delta x_i}{\Delta x_{i\pm 1} + \Delta x_i}, \tag{61}
$$

and

$$
\Delta \ell_{xy} = \Delta x_i\ [\Delta y_j + \frac{1}{2}(\Delta y_{j+1} + \Delta y_{j-1})]. \tag{62}
$$

Approximation of the remaining derivatives in two- and three-dimensional problems can be easily obtained by cyclical substitution.

The approximation of the diffusive component of equation (45) leads to a set of coefficients corresponding to communication of the gridblock (i, j, k) with its neighboring gridblocks. The coefficient for Ψ_{ijk} is

$$
\sigma_0 = -(G^+_x + G^-_x + G^+_y + G^-_y + G^+_z + G^-_z), \tag{63}
$$

$$
\text{for } \Psi_{i-1,j,k}: \quad \sigma_1 = G^-_x - a_{1j}\ G^+_{yx} + b_{2j}\ G^-_{yx} - a_{1k}\ G^+_{zx} + b_{2k}\ G^-_{zx}, \tag{64}
$$

$$
\text{for } \Psi_{i+1,j,k}: \quad \sigma_2 = G^+_x + G^-_x - \sigma_1, \tag{65}
$$

$$
\text{for } \Psi_{i,j-1,k}: \quad \sigma_3 = G^-_y - a_{1i}\ G^+_{xy} + b_{2i}\ G^-_{xy} - a_{1k}\ G^+_{zy} + b_{2k}\ G^-_{zy}, \tag{66}
$$

$$
\text{for } \Psi_{i,j+1,k}: \quad \sigma_4 = G^+_y + G^-_y - \sigma_3, \tag{67}
$$

$$
\text{for } \Psi_{i,j,k-1}: \quad \sigma_5 = G^-_z - a_{1i}\ G^+_{xz} + b_{2i}\ G^-_{xz} - a_{1j}\ G^+_{yz} + b_{2j}\ G^-_{yz}, \tag{68}
$$

$$
\text{for } \Psi_{i,j,k+1}: \quad \sigma_6 = G^+_z + G^-_z - \sigma_5, \tag{69}
$$

$$
\text{for } \Psi_{i-1,j-1,k}: \quad \sigma_7 = b_{1i}\ G^-_{xy} + b_{1j}\ G^-_{yx}, \tag{70}
$$

$$\text{for } \Psi_{i-1,j+1,k}: \quad \sigma_8 = -b_{1i}\, G^-_{xy} - a_{2j}\, G^+_{yx}, \tag{71}$$

$$\text{for } \Psi_{i+1,j-1,k}: \quad \sigma_9 = -a_{2i}\, G^+_{xy} - b_{1j}\, G^-_{yx}, \tag{72}$$

$$\text{for } \Psi_{i+1,j+1,k}: \quad \sigma_{10} = a_{2i}\, G^+_{xy} + a_{2j}\, G^+_{yx}, \tag{73}$$

$$\text{for } \Psi_{i-1,j,k-1}: \quad \sigma_{11} = b_{1i}\, G^-_{xz} + b_{1k}\, G^-_{zx}, \tag{74}$$

$$\text{for } \Psi_{i-1,j,k+1}: \quad \sigma_{12} = -b_{1i}\, G^-_{xz} - a_{2k}\, G^+_{zx}, \tag{75}$$

$$\text{for } \Psi_{i+1,j,k-1}: \quad \sigma_{13} = -a_{2i}\, G^+_{xz} - b_{1k}\, G^-_{zx}, \tag{76}$$

$$\text{for } \Psi_{i+1,j,k+1}: \quad \sigma_{14} = a_{2i}\, G^+_{xz} + a_{2k}\, G^+_{zx}, \tag{77}$$

$$\text{for } \Psi_{i,j-1,k-1}: \quad \sigma_{15} = b_{1j}\, G^-_{yz} + b_{1k}\, G^-_{zy}, \tag{78}$$

$$\text{for } \Psi_{i,j-1,k+1}: \quad \sigma_{16} = -b_{1j}\, G^-_{yz} - a_{2k}\, G^+_{zy}, \tag{79}$$

$$\text{for } \Psi_{i,j+1,k+1}: \quad \sigma_{17} = -a_{2j}\, G^+_{yz} - b_{1k}\, G^-_{zy}, \tag{80}$$

and

$$\text{for } \Psi_{i,j+1,k+1}: \quad \sigma_{18} = a_{2j}\, G^+_{yz} + a_{2k}\, G^+_{zy}. \tag{81}$$

5.3. Treatment of Boundaries

The treatment of the pressure boundaries has been discussed in detail by *Moridis and Reddell* [1991*a*]. Here we concentrate on the treatment of the Ψ boundaries. If the gridblocks under consideration are not located at the corners or edges of the domain, there are two possilities (Figure 2):

1. A Dirichlet type (hereafter referred to as D-type) boundary at $x = 0$: $i = 1$ and $j > 1$ (Figure 2a). Then no modification is needed in the coefficients developed in the approximation of the derivatives.

2. A Neuman-type (hereafter referred to as N-type) boundary boundary at $x = 0$: $i = 1$ and $j > 1$ (Figure 2b), with $(\frac{\partial \Psi}{\partial x})_{i-\frac{1}{2}} = f_{x0}$. Then the approximation of $\frac{\partial}{\partial y}\left(D_{yy}\,\frac{\partial \Psi}{\partial y}\right)$ is unaffected but

$$\frac{\partial}{\partial x}\left(D_{xx}\,\frac{\partial \Psi}{\partial x}\right) \simeq \frac{\left(D_{xx}\,\dfrac{\partial \Psi}{\partial y}\right)_{i+\frac{1}{2}} - (D_{xx})_{i-\frac{1}{2}}\; f_{x0}}{\Delta x_i}$$

$$= G_x^{+}(\Psi_{i+1} - \Psi_i) - F_{x0}, \quad F_{x0} = f_{x0}\,\frac{(D_{xx})_{i-\frac{1}{2}}}{\Delta x_i} \tag{82}$$

where G_x^{+} are as in equation (60), and $G_x^{-} = 0$. The cross derivative

$$\frac{\partial}{\partial x}\left(D_{xy}\,\frac{\partial \Psi}{\partial y}\right) \simeq \frac{\left(D_{xy}\,\dfrac{\partial \Psi}{\partial y}\right)_{i+\frac{1}{2},j} - \left(D_{xy}\,\dfrac{\partial \Psi}{\partial y}\right)_{i,j}}{\Delta x_i}, \tag{83}$$

which results in equations (60) and (61) with the difference

$$b_{1i} = 0 \qquad \text{and} \qquad b_{2i} = 1. \tag{84}$$

Finally, the cross derivative

$$\frac{\partial}{\partial y}\left(D_{xy}\,\frac{\partial \Psi}{\partial x}\right) \simeq \frac{\left(D_{xy}\,\dfrac{\partial \Psi}{\partial x}\right)_{j+\frac{1}{2}} - \left(D_{xy}\,\dfrac{\partial \Psi}{\partial x}\right)_{j-\frac{1}{2}}}{\Delta y_j}$$

$$\begin{aligned} =& G_{yx}^{2+}\;\left(a_{1j}\;\Psi_{i+1,j} + a_{2j}\;\Psi_{i+1,j+1} - a_{1j}\;\Psi_{i,j} - a_{2j}\;\Psi_{i,j+1}\right) \\ -& G_{yx}^{2-}\;\left(b_{1j}\;\Psi_{i+1,j-1} + b_{2j}\;\Psi_{i+1,j} - b_{1j}\;\Psi_{i,j-1} - b_{2j}\;\Psi_{i,j}\right), \end{aligned} \tag{85}$$

where

$$G_{yx}^{2\pm} = \frac{(D_{xy})_{j\pm\frac{1}{2}}}{\Delta \ell'_{yx}}, \qquad \Delta \ell'_{yx} = 0.5\;\Delta y_j\;(\Delta x_i + \Delta x_{i+1}), \tag{86}$$

and the terms a_{1j}, a_{2j}, b_{1j}, b_{2j} remain as defined in (61). The coefficients of equations (63) through (81) are then appropriately adjusted.

The approximation of the boundary conditions becomes more complicated at the corner and edge gridblocks. Working with an (i,j) system in (x,y), we can identify the following four additional possibilities at $(i=1, j=1)$ in Figure 2:

3. A D-type boundary at $x=0$, and a D-type boundary at $y=0$ (Figure 2c). In this case the approximation of $\frac{\partial}{\partial x}\left(D_{xx}\,\frac{\partial\Psi}{\partial x}\right)$ and $\frac{\partial}{\partial y}\left(D_{yy}\,\frac{\partial\Psi}{\partial y}\right)$ are given by substitution in equation (58). The cross derivative

$$\begin{aligned}\frac{\partial}{\partial x}\left(D_{xy}\,\frac{\partial\Psi}{\partial y}\right) \simeq & \frac{\left(D_{xy}\,\dfrac{\partial\Psi}{\partial y}\right)_{i+\frac{1}{2}} - \left(D_{xy}\,\dfrac{\partial\Psi}{\partial y}\right)_{i-\frac{1}{2}}}{\Delta x_i} \\ =& G_{xy}^{+}\ \left(a_{1i}\ \Psi_{i,j+1} + a_{2i}\ \Psi_{i+1,j+1} - a_{1i}\ \Psi_{i,j-1} - a_{2i}\ \Psi_{i+1,j-1}\right) \\ -& G_{xy}^{2-}\ \left(b_{1i}\ \Psi_{i-1,j+1} + b_{2i}\ \Psi_{i,j+1} - b_{1i}\ \Psi_{i-1,j} - b_{2i}\ \Psi_{i,j}\right),\end{aligned} \tag{87}$$

and

$$\begin{aligned}\frac{\partial}{\partial y}\left(D_{xy}\,\frac{\partial\Psi}{\partial x}\right) \simeq & \frac{\left(D_{xy}\,\dfrac{\partial\Psi}{\partial x}\right)_{j+\frac{1}{2}} - \left(D_{xy}\,\dfrac{\partial\Psi}{\partial x}\right)_{j-\frac{1}{2}}}{\Delta y_j} \\ =& G_{yx}^{+}\ \left(a_{1j}\ \Psi_{i+1,j} + a_{2j}\ \Psi_{i+1,j+1} - a_{1j}\ \Psi_{i-1,j} - a_{2j}\ \Psi_{i-1,j+1}\right) \\ -& G_{yx}^{2-}\ \left(b_{1j}\ \Psi_{i+1,j-1} + b_{2j}\ \Psi_{i+1,j} - b_{1j}\ \Psi_{i,j-1} - b_{2j}\ \Psi_{i,j}\right).\end{aligned} \tag{88}$$

4. A D-type boundary at $x=0$, and a N-type boundary at $y=0$ (Figure 2d). Then equation (58) approximates $\frac{\partial}{\partial x}\left(D_{xx}\,\frac{\partial\Psi}{\partial x}\right)$, and equation (82) approximates $\frac{\partial}{\partial y}\left(D_{yy}\,\frac{\partial\Psi}{\partial y}\right)$. The cross derivative

$$\begin{aligned}\frac{\partial}{\partial x}\left(D_{xy}\,\frac{\partial\Psi}{\partial y}\right) \simeq & \frac{\left(D_{xy}\,\dfrac{\partial\Psi}{\partial y}\right)_{i+\frac{1}{2}} - \left(D_{xy}\,\dfrac{\partial\Psi}{\partial y}\right)_{i-\frac{1}{2}}}{\Delta x_i} \\ =& G_{xy}^{2+}\ \left(a_{1i}\ \Psi_{i,j+1} + a_{2i}\ \Psi_{i+1,j+1} - a_{1i}\ \Psi_{i,j} - a_{2i}\ \Psi_{i+1,j}\right) \\ -& G_{xy}^{2-}\ \left(b_{1i}\ \Psi_{i-1,j+1} + b_{2i}\ \Psi_{i,j+1} - b_{1i}\ \Psi_{i-1,j} - b_{2i}\ \Psi_{i,j}\right).\end{aligned} \tag{89}$$

Finally, $\frac{\partial}{\partial y}(D_{xy}\,\frac{\partial\Psi}{\partial x})$ is approximated using equations (83) and (84).

5. A N-type boundary at $x=0$, and a D-type boundary at $y=0$ (Figure 2e). Then equation (1) approximates $\frac{\partial}{\partial y}\left(D_{yy}\,\frac{\partial\Psi}{\partial y}\right)$ and equation (82) approximates $\frac{\partial}{\partial x}\left(D_{xx}\,\frac{\partial\Psi}{\partial x}\right)$.

We use equations (83) and (84) to approximate $\frac{\partial}{\partial x}(D_{xy}\ \frac{\partial \Psi}{\partial y})$, and equation (85) for $\frac{\partial}{\partial y}(D_{xy}\ \frac{\partial \Psi}{\partial x})$.

6. A N-type boundary at $x = 0$, and a N-type boundary at $y = 0$ (Figure 2f). Equation (82) applies for the approximation of $\frac{\partial}{\partial y}\left(D_{yy}\ \frac{\partial \Psi}{\partial y}\right)$ and $\frac{\partial}{\partial x}\left(D_{xx}\ \frac{\partial \Psi}{\partial x}\right)$. We use equations (83) and (84) to approximate $\frac{\partial}{\partial x}(D_{xy}\ \frac{\partial \Psi}{\partial y})$, and equation (85) for $\frac{\partial}{\partial y}(D_{xy}\ \frac{\partial \Psi}{\partial x})$. The cross derivative

$$\begin{aligned}\frac{\partial}{\partial x}\left(D_{xy}\ \frac{\partial \Psi}{\partial y}\right) \simeq & \frac{\left(D_{xy}\ \frac{\partial \Psi}{\partial y}\right)_{i+\frac{1}{2}} - \left(D_{xy}\ \frac{\partial \Psi}{\partial y}\right)_{i}}{\Delta x_i} \\ =& G_{xy}^{2+}\ \left(a_{1i}\ \Psi_{i,j+1} + a_{2i}\ \Psi_{i+1,j+1} - a_{1i}\ \Psi_{i,j-1} - a_{2i}\ \Psi_{i+1,j-1}\right) \\ -& G_{xy}^{2-}\ \left(\Psi_{i,j+1} - \Psi_{i,j}\right).\end{aligned} \tag{90}$$

Similarly, substituting (x, y, i, j) for (y, x, j, i) in (90) yields the approximation of the term $\frac{\partial}{\partial y}(D_{xy}\ \frac{\partial \Psi}{\partial x})$.

The other type of boundary that needs to be examined is the mixed-type, hereafter referred to as M-type. We can identify two additional cases:

7. M-boundary at $x = 0$ $(i = 1)$, with D-type for $1 < j < j_m$ and N-type for $j_m \leq j < M_Y$ (Figures 2g and 2h). At $(i = 1, j = j_m)$, this boundary gridblock is treated exactly like the one described in case 5.

The gridblock at $(i = 1, j = j_m - 1)$, i.e. the first D-type boundary gridblock has to be treated differently. In the case the approximation of $\frac{\partial}{\partial x}\left(D_{xx}\ \frac{\partial \Psi}{\partial x}\right)$ and $\frac{\partial}{\partial y}\left(D_{yy}\ \frac{\partial \Psi}{\partial y}\right)$ is accomplished by using equation (58). However,

$$\begin{aligned}\frac{\partial}{\partial x}\left(D_{xy}\ \frac{\partial \Psi}{\partial y}\right) \simeq & \frac{\left(D_{xy}\ \frac{\partial \Psi}{\partial y}\right)_{i+\frac{1}{2}} - \left(D_{xy}\ \frac{\partial \Psi}{\partial y}\right)_{i-\frac{1}{2}}}{\Delta x_i} \\ =& G_{xy}^{+}\ \left(a_{1i}\ \Psi_{i,j+1} + a_{2i}\ \Psi_{i+1,j+1} - a_{1i}\ \Psi_{i,j-1} - a_{2i}\ \Psi_{i+1,j-1}\right) \\ -& G_{xy}^{3-}\ \left(b_{1i}\ \Psi_{i-1,j} + b_{2i}\ \Psi_{i,j} - b_{1i}\ \Psi_{i-1,j-1} - b_{2i}\ \Psi_{i,j-1}\right),\end{aligned} \tag{91}$$

where

$$G_{xy}^{3\pm} = (D_{xy})_{i\pm\frac{1}{2}}\ \frac{2}{\Delta x_i(\Delta y_j + \Delta y_{j-1})}, \tag{92}$$

and the terms a_{1j}, a_{2j}, b_{1j}, b_{2j} remain as defined in (61). Finally,

$$\begin{aligned}\frac{\partial}{\partial y}\left(D_{xy}\,\frac{\partial\Psi}{\partial x}\right) \simeq & \frac{\left(D_{xy}\,\frac{\partial\Psi}{\partial x}\right)_{i+\frac{1}{2}} - \left(D_{xy}\,\frac{\partial\Psi}{\partial x}\right)_{i-\frac{1}{2}}}{\Delta y_j} \\ =& G_{yx}^{2+}\ \left(a_{1j}\ \Psi_{i+1,j} + a_{2j}\ \Psi_{i+1,j+1} - a_{1j}\ \Psi_{i,j} - a_{2j}\ \Psi_{i,j+1}\right) \\ -& G_{yx}^{-}\ \left(b_{1j}\ \Psi_{i+1,j-1} + b_{2j}\ \Psi_{i+1,j} - b_{1j}\ \Psi_{i-1,j-1} - b_{2j}\ \Psi_{i-1,j}\right).\end{aligned} \tag{93}$$

8. M-boundary at $x = 0$ $(i = 1)$, with N-type for $1 < j \geq j_m$ and D-type for $j_m < j < M_Y$ (Figures 2i and 2j). At $(i = 1, j = j_m)$ equation (58) approximates $\frac{\partial}{\partial y}\left(D_{yy}\,\frac{\partial\Psi}{\partial y}\right)$, and $\frac{\partial}{\partial x}\left(D_{xx}\,\frac{\partial\Psi}{\partial x}\right)$ is discretized using (82). We approximate $\frac{\partial}{\partial x}(D_{xy}\,\frac{\partial\Psi}{\partial y})$ using (83) and (84), and $\frac{\partial}{\partial y}(D_{xy}\,\frac{\partial\Psi}{\partial x})$ using (85).

The treatment of the gridblock $(i = 1, j = j_m + 1)$, i.e. the first D-type boundary gridblock, is the same as in case 3.

5.4. Advection-Related Derivatives in the Transport Equation

The greatest challenge is the approximation of the first-order spatial derivative in the advection terms $\frac{\partial(V\Psi)}{\partial x}$ in equation (45). We investigated two differencing operators: (a) a single-point upstream, and (b) the higher order method of *Saad et al.* [1990]. At node i in the 1-D system $(x_1 \equiv x)$ of Figure 3 both differencing operators are defined by the general expression

$$\left[\frac{\partial(V\ \Psi)}{\partial x}\right]_i = \frac{V_{i+1/2}\ \Psi_{i+1/2} - V_{i-1/2}\ \Psi_{i-1/2}}{\Delta x_i}. \tag{94}$$

The subscripts $_{i\pm1/2}$ indicate values of the corresponding terms at the block interfaces. Using Darcy's law, the terms $V_{i\pm1/2}$ are readily available from the solution of the discretized equation (41).

In the single point upstream weighting method,

$$\Psi_{i\pm\frac{1}{2}} = \begin{cases} \Psi_i & \text{if flow is from } i \text{ to } i \pm 1 \\ \Psi_{i\pm1} & \text{if flow is from } i \pm 1 \text{ to } i\ . \end{cases} \tag{95}$$

The direction of the flow is provided by the sign of $\Delta p_{\pm} = p_{i\pm1} - p_i$, where $p = P - \rho g h$ is the potential. A positive sign indicates flow from $i \pm 1$ to i. This scheme provides only a first order approximation, and may introduce significant numerical diffusion [*Lantz*, 1971].

The higher order scheme of *Saad et al.* [1990] is a modification of the differencing operator suggested by *Leonard* [1979]. For a variable grid size (not allowed in the Leonard scheme), and for $p_{i-1} \leq p_i \leq i_{i+1}$ (Figure 3a),

$$\Psi_{i+1/2} = \Psi_{i+1} + 2\ A_{i+1}\ (\Psi_i - \Psi_{i+1}) + B_{i+1}\ (\Psi_{i+1} - \Psi_{i+2}), \tag{96}$$

and

$$\Psi_{i-1/2} = \Psi_i + 2\ A_i\ (\Psi_{i-1} - \Psi_i) + B_i\ (\Psi_i - \Psi_{i+1}), \tag{97}$$

where

$$A_i = \frac{\Delta x_i}{3(\Delta x_i + \Delta x_{i-1})} \quad \text{and} \quad B_i = \frac{\Delta x_i}{3(\Delta x_i + \Delta x_{i+1})}. \tag{98}$$

For $p_{i-1} \geq p_i \geq p_{i+1}$ (Figure 3b),

$$\Psi_{i+1/2} = \Psi_i + A_i\ (\Psi_i - \Psi_{i-1}) + 2\ B_i\ (\Psi_{i+1} - \Psi_i), \tag{99}$$

and

$$\Psi_{i-1/2} = \Psi_{i-1} + A_{i-1}\ (\Psi_{i-1} - \Psi_{i-2}) + 2\ B_{i-1}\ (\Psi_i - \Psi_{i-1}). \tag{100}$$

For $p_{i-1} \geq p_i$ and $p_i \leq p_{i+1}$ (Figure 3c), equations (96) and (100) are used to determine $\Psi_{i+1/2}$ and $\Psi_{i-1/2}$ respectively. Finally, when $p_{i-1} \leq p_i$ and $p_i \geq p_{i+1}$, equations (97) and (99) are used for $p_{i-1/2}$ and $p_{i+1/2}$ respectively.

These approximations are derived using a conservative-control-volume formulation [*Saad et al.*,1990], with gridblock face values of Ψ expressed in terms of three nodal values: the nodal value at i, plus two upstream values.. When the water velocities at the opposite sides of a gridblock have the same sign (Figures 3a and 3b) , information from 4 nodes is used. For diverging flow (Figure 3c) three centrally located nodes are needed. For converging flow (Figure 3d), the approximation involves five nodes symetrically arranged

on both sides of node i. Extension to two or three dimensions is entirely analogous (Figure 4). The variable-grid formulation is second-order correct, and as such more accurate than the single-point upstream approximation, which is zero-order correct when used with a variable grid size. For a uniform grid spacing, the scheme is third-order correct.

Applying the procedures described above, the discretization of equations (41), (45), and (46) in the Laplace space yields three general algebraic equations valid in each of the M gridblocks of the space domain. Depending on the appropriate number of applicable equations per gridblock, the number of the resulting algebraic equations $N = N_e \times M$, where N_e is the number of simultaneous equations per gridblock.

6. Step 3: The Solution in the Laplace Space

The resulting algebraic equations may be written in a general matrix form as:

$$\widehat{\mathbf{T}}\,\vec{\mathbf{X}} = \vec{\mathbf{B}}\,, \tag{101}$$

where $\widehat{\mathbf{T}}$ is the coefficient matrix, $\vec{\mathbf{X}}$ is the vector of the unknowns, and $\vec{\mathbf{B}}$ is the composite vector of knowns. The computation of $\widehat{\mathbf{T}}$ and $\vec{\mathbf{B}}$ necessitates values for the λ parameter of the Laplace space. These are provided by the two schemes: the Stehfest algorithm [*Stehfest*,1970*a*; 1970*b*], and the DeHoog method [*DeHoog et al.*,1982]. For a desired observation time t, the λ in the Stehfest algorithm is real and given by

$$\lambda_\nu = \frac{\ln 2}{t} \cdot \nu, \qquad \nu = 1, \ldots, N_S \tag{102}$$

where N_S is the number of summation terms in the algorithm and is an even number. In the DeHoog method, λ is a complex number given by *Crump* [1974] and *Sudicky* [1989] as

$$\lambda_\nu = \lambda_0 + \frac{\nu\pi}{\Omega}\, i, \qquad \lambda_0 = \mu - \frac{\ln(E_R)}{2T}, \qquad \nu = 1, \ldots, N_H \tag{103}$$

where 2Ω is the period of the Fourier series approximating the inverse function in the interval $[0, 2\Omega]$, $i = \sqrt{-1}$, and $N_H = 2M_H + 1$ is an odd number. A thorough discussion of

the terms μ and E_R and their significance can be found in *Sudicky* [1989]. As is discussed in *Moridis* [1995], excellent results are obtained when $\mu = 0$, $10^{-10} \leq E_R \leq 10^{-8}$, and $0.9\ t_{max} \leq \Omega \leq 1.1\ t_{max}$, where t_{max} is the maximum simulation time.

The vectors

$$\vec{\mathbf{X}} = \left[\vec{\mathbf{X}}_1, \vec{\mathbf{X}}_2, \ldots, \vec{\mathbf{X}}_\kappa, \ldots, \vec{\mathbf{X}}_M\right]^{\mathrm{T}}, \quad \vec{\mathbf{B}} = \left[\vec{\mathbf{B}}_1, \vec{\mathbf{X}}_2, \ldots, \vec{\mathbf{B}}_\kappa, \ldots, \vec{\mathbf{B}}_M\right]^{\mathrm{T}}, \tag{104}$$

where the vectors $\vec{\mathbf{X}}_\kappa$ and $\vec{\mathbf{B}}_\kappa$ correspond to the unknowns and right-hand side at each gridblock. Their length is a function of the number of the unknowns and the type of the Laplace parameter λ. The quantities Φ, Ψ and Υ assume the real or complex type of λ.

The three-element vector $\vec{\mathbf{X}}_\kappa = [\Phi, \Psi, \Upsilon]_\kappa^T$ applies when all three equations are solved simultaneously, and corresponds to the three-element vector $\vec{\mathbf{B}}_\kappa = [B_P, B_X, B_S]_\kappa^T$. When (a) the effect of the solute concentration on water density is measurable but does not violate the linearity assumption and (b) adsorption is reversible or neglected, the two element vector $\vec{\mathbf{X}}_\kappa = [\Phi, \Psi]_\kappa^T$ applies, and $\vec{\mathbf{B}}_\kappa = [B_P, B_X]_\kappa^T$. Single element vectors apply to very dilute solutions where the water density is not affected. Then equation (41) is a function of Φ only and is solved first to provide the V's needed in (45). In the presence of non-linear and/or irreversible adsorption, equations (45) and (46) need to be solved simultaneously. Then $\vec{\mathbf{X}}_\kappa = [\Psi, \Upsilon]_\kappa^T$ is a two-element vector, and $\vec{\mathbf{B}}_\kappa = [B_X, B_S]_\kappa^T$.

When the single-point upstream scheme is used, the κth block row of matrix $\widehat{\mathbf{T}}$, associated with the gridblock $\kappa = (\kappa_1, \kappa_2, \kappa_3)$, is

$$\underbrace{\overbrace{\mathbf{T}_{\kappa_1-1}\ \mathbf{0}\cdots\mathbf{0}\ \ \mathbf{T}_{\kappa_2-1}\ \mathbf{0}\cdots\mathbf{0}\ \ \mathbf{T}_{\kappa_3-1}}^{M_3M_2}\ \ \mathbf{T}_\kappa\ \ \underbrace{\mathbf{T}_{\kappa_3+1}\ \mathbf{0}\cdots\mathbf{0}\ \ \mathbf{T}_{\kappa_2+1}}_{M_3}\ \mathbf{0}\cdots\mathbf{0}\ \ \mathbf{T}_{\kappa_1+1}}_{2M_3M_2+1} \tag{105}$$

when $M_1 \geq M_2 \geq M_3$, indicating a bandwidth $B_W = 2\ (M_3 \times M_2 + 1)\ N_e - 1$. For real λ, $N_e = 1$, 2, or 3; for complex λ, $N_e = 2$, 3, or 6. When the higher-order scheme of *Saad et al.* [1990] is used, the left half of the κ-th block row of matrix $\mathbf{T}_\kappa$, associated with the

grid-block $\kappa = (\kappa_1, \kappa_2, \kappa_3)$, is:

$$\underbrace{\mathbf{T}_{\kappa_1-2}\ \mathbf{0}\cdots\mathbf{0}\ \overbrace{\mathbf{T}_{\kappa_1-1}\ \mathbf{0}\cdots\mathbf{0}\ \underbrace{\mathbf{T}_{\kappa_2-2}\ \mathbf{0}\cdots\mathbf{0}\ \overbrace{\mathbf{T}_{\kappa_2-1}\ \mathbf{0}\cdots\mathbf{0}\ \mathbf{T}_{\kappa_3-2}\ \mathbf{T}_{\kappa_3-1}}^{M_3}}_{2M_2}}^{M_3M_2}\ \mathbf{T}_{\kappa}}_{2M_3M_2+1} \tag{106}$$

when $M_1 \geq M_2 \geq M_3$, indicating a bandwidth $B_W = 2\ (2\ M_3 \times M_2 + 1)\ N_e - 1$, i.e. almost double that of equation (105). In both cases there is symmetry to the right and left of the central block-matrix $\mathbf{T}$ with regard to the positions of the block-matrices.

The solution of equation (101) returns a set of N_S or N_H vectors of the unknown $\vec{\mathbf{X}}$'s as

$$\vec{\mathbf{X}}_\nu = \vec{\mathbf{X}}(\lambda_\nu) = \left[\widehat{\mathbf{T}}(\lambda_\nu)\right]^{-1} \vec{\mathbf{B}}(\lambda_\nu)\ , \quad \nu = 1, \ldots, N_S \text{ or } N_H. \tag{107}$$

To obtain a solution at a time t, all vectors $\vec{\mathbf{X}}_\nu$, $\nu = 1, \ldots, N_S$ or N_H are needed, i.e. the system of simultaneous equations has to be solved N_S or N_H times.

When using the DeHoog method, the matrix equation (101) involves complex numbers and Φ, Ψ and Υ are complex. The easiest and simplest way to solve (101) is to use the complex arithmetic operations available to FORTRAN. However, this is a very inefficient approach because operations on complex numbers are very slow.

A much faster execution is achieved by splitting each one of the discretized equations into two equations containing the real and the imaginary parts of f_P, f_X, and f_S. Depending on the number of initial simultaneous equations, this approach uses strictly real computer arithmetic. This approach requires determination of the unknowns Φ_R, Φ_I, Ψ_R, Ψ_I, Υ_R and Υ_I, where

$$\Phi = \Phi_R + i\Phi_I, \quad \Psi = \Psi_R + i\Psi_I, \quad \Upsilon = \Upsilon_R + i\Upsilon_I, \tag{108}$$

and the subscripts $_R$ and $_I$ denote the real and imaginary parts respectively. This yields 6, 4, or 2 equations per gridblock and requires significantly less execution time than

using complex arithmetic. For example, if equations (41), (45), and (46) must be solved simultaneously, at each gridblock κ the vectors of the unknowns and the right-hand sides respectively are

$$\vec{\mathbf{X}}_\kappa = \begin{pmatrix} \Phi_R \\ \Phi_I \\ \Psi_R \\ \Psi_I \\ \Upsilon_R \\ \Upsilon_I \end{pmatrix}_\kappa \quad \text{and} \quad \vec{\mathbf{B}}_\kappa = \begin{pmatrix} \mathrm{Re}\{B_P\} \\ \mathrm{Im}\{B_P\} \\ \mathrm{Re}\{B_X\} \\ \mathrm{Im}\{B_X\} \\ \mathrm{Re}\{B_S\} \\ \mathrm{Im}\{B_S\} \end{pmatrix}_\kappa . \tag{109}$$

When the DeHoog method is used, the off-diagonal block-submatrices $\mathbf{T}_{\kappa_1\pm1}$, $\mathbf{T}_{\kappa_1\pm2}$, $\mathbf{T}_{\kappa_2\pm1}$, $\mathbf{T}_{\kappa_2\pm2}$, $\mathbf{T}_{\kappa_3\pm1}$, and $\mathbf{T}_{\kappa_3\pm2}$ have non-zero elements on their main diagonals only. If the same held true for the diagonal submatrix $\mathbf{T}_\kappa$, then the equations of the real and the imaginary parts would be completely independent, and, therefore, could be solved separately. This, however, is not possible due to the presence of the products $K_{2P}\Phi$, $K_{2X}\Psi$ in equation (41), $F_{1P}\Phi$, $F_{3X}\Psi$ in (45), and $G_{1P}\Phi$, $G_{1X}\Psi$ in (46). These products involve multiplications of the complex Φ and Ψ with the complex λ, and create non-zero entries off the main diagonal of submatrix $\mathbf{T}_\kappa$.

Due to the need to compute both the real and imaginary parts of the unknown dependent variables, for the same problem the DeHoog method increases both (a) the number N of equations in (101) and (b) the bandwidth B_W of the matrix to twice those of the Stehfest formulation. Compared to the Stehfest algorithm, the DeHoog method creates a coefficient matrix $\widehat{\mathbf{T}}$ four times as large, and thus requires four times the storage. The corresponding increase in execution time depends on the type of the solver. For an efficient direct solver the execution time is expected to increase by a factor of 8 [*Price and Coats*,1974]. Generalizations are harder for iterative solvers, but an efficient conjugate gradient solver is expected to increase the execution time by a minimum factor of 2.6 [*Moridis and Pruess*,1995].

If the effect of the solute on the water density is negligible and the flow equation can be solved separately, significant savings in storage and execution time can be realized by

using the Stehfest algorithm because it has been shown that for flow problems there is no difference in the performance of the DeHoog and the Stehfest algorithms [*Moridis*,1992]. The resulting Darcian velocities V can then be used in the solution of the transport and adsorbate equations. A more thorough discussion on the relative merits of the DeHoog and Stehfest formulations is presented in the second paper of this series [*Moridis*,1995].

7. Step 4: The Iterative Process

If the velocity field is time-invariant and the fluid density is not affected by the presence of solutes, there is no need for inner iterations and the LTFD solution proceeds directly to Step 5. Under all other conditions, the linearization of the non-linearities encountered in the extension of the LTFD method to the solution of the solute transport problem necessitates an iteration procedure analogous to the treatment of such non-linearities in standard Finite Differences or Finite Elements. The procedure is described as follows:

1. The linearized elements of the initial matrix $[\widehat{\mathbf{T}}^{-1}]_0$ and the vector $[\vec{\mathbf{B}}]_0$ are calculated using the initial values χ_0 as an approximation of the required time averaged quantities $\overline{\chi}$ (equation (15)). An initial solution $[\vec{\mathbf{X}}]_1$ is obtained from equation (101).
2. From $\vec{\mathbf{X}}_1$ and the properties of Laplace transforms, the relevant time averaged quantities $\overline{\chi}$ are calculated as

$$\overline{\chi} = \frac{1}{t}\int_0^t \chi \, dt = \frac{1}{t}\,\mathcal{L}^{-1}\left\{\frac{\widehat{\chi}}{\lambda}\right\}, \tag{110}$$

   where $\widehat{\chi} = \mathcal{L}\{\chi\}$.
3. Using the $\overline{\chi}$ and the adjusted gradients from step 2, the elements of the updated matrix $[\widehat{\mathbf{T}}^{-1}]_1$ and vector $[\vec{\mathbf{B}}]_1$ are obtained.
4. An improved solution $[\vec{\mathbf{X}}]_2$ is obtained using the updated $[\widehat{\mathbf{T}}^{-1}]_1$ and $[\vec{\mathbf{B}}]_1$.
5. Steps 2 through 4 are repeated until a desired convergence criterion is met. In our experience convergence is very rapid, and seldom requires more than 3-4 iterations. The solution in time $\vec{\mathbf{U}}(t)$ is then obtained by inverting the converged solution $\vec{\mathbf{X}}$ in the

following step. It must be pointed out that the linearization and the corresponding inner iterations will produce an accurate solution only as long as the underlying approximations are valid. In our experience this holds true if the change in the water density does not exceed 1.5%, i.e. 50% higher than in the traditional Boussinesq assumptions.

8. Step 5: The Numerical Inversion of the Laplace Solution

The unknown vector $\vec{\mathbf{U}}$ at any time t is obtained by by numerically inverting the Laplace space solutions $\vec{\mathbf{X}}(\lambda_\nu)$. When using the Stehfest algorithm, the unknowns $U \equiv P, X, X_s$ at a point κ and a time t are obtained from

$$[U(t)]_\kappa = \frac{\ln 2}{t} \sum_{\nu=1}^{N_S} W_\nu \; [X(\lambda_\nu)]_\kappa \; , \tag{111}$$

where

$$W_\nu = (-1)^{\frac{N_S}{2}+\nu} \sum_{k=\frac{1}{2}(\nu+1)}^{\min\{\nu,\frac{N_S}{2}\}} \frac{k^{\frac{N_S}{2}}(2k!)}{(\frac{N_S}{2}-k)!k!(k-1)!(\nu-k)!(2k-\nu)!} \; . \tag{112}$$

Although the accuracy of the method is theoretically expected to improve with increasing N_S, *Stehfest* [1970*a*; 1970*b*] showed that with increasing N_S the number of correct significant figures inreases linearly at first and then, due to roundoff errors, decreases linearly. He determined that the optimum N_S was 10 for single precision variables (8 significant figures) and 18 for double precision variables (16 significant figures). However, *Moridis and Reddell* [1991; 1991*a*; 1991*c*] reported that LTFD seems to be insensitive to N_S for $6 \leq N_S \leq 20$.

The inversion of the Laplace space solution obtained with the DeHoog method is far more complicated. The solution $\vec{\mathbf{U}}$ at a time t is given by

$$[U(t)]_\kappa = \frac{1}{\Omega} \exp(\lambda_0 t) \; \mathrm{Re}\left\{ \left[\frac{A_{2M}}{B_{2M}} \right]_\kappa \right\}, \tag{113}$$

where

$$A_n = A_{n-1} + d_n \; z \; A_{n-2}, \quad B_n = B_{n-1} + d_n \; z \; B_{n-2}, \quad n = 1, \ldots, 2M, \tag{114}$$

and $A_{-1} = 0$, $A_0 = d_0$, $B_{-1} = B_0 = 1$;

$$d_0 = a_0, \quad d_{2m-1} = -q_m^{(0)}, \quad d_{2m} = -e_m^{(0)}, \qquad m = 1, \ldots, M, \tag{115}$$

$$\begin{aligned} \ell = 1, \ldots, M, \qquad & e_\ell^{(k)} = q_\ell^{(k+1)} - q_\ell^{(k)} + e_{\ell-1}^{(k+1)}, \qquad k = 0, \ldots, 2M - 2\ell \\ \text{for } \ell = 2, \ldots, M, \qquad & q_\ell^{(k)} = q_{\ell-1}^{(k+1)}\ e_{\ell-1}^{(k+1)} / e_{\ell-1}^{(k)}, \qquad k = 0, \ldots, 2M - 2\ell - 1, \end{aligned} \tag{116}$$

$$e_0^{(k)} = 0 \text{ for } k = 0, \ldots, 2M \quad \text{and} \quad q_1^{(k)} = a_{k+1}/a_k \text{ for } k = 0, \ldots, 2M - 1, \tag{117}$$

and

$$a_0 = \frac{1}{2} X(\lambda_0), \quad a_k = X(\lambda_k) \quad \text{and} \quad z = \exp(j\pi t/\Omega). \tag{118}$$

A further acceleration is obtained if on the last evaluation of the recurrence relations $d_{2M}\ z$ is repaced by $R_{2M}(z)$,

$$R_{2M}(z) = -h_{2M} \left[1 - \sqrt{(1 + d_{2M}\ z/h_{2M})}\right], \quad h_{2M} = \frac{1}{2}[1 + z\ (d_{2M-1} - d_{2M})], \tag{119}$$

giving

$$\widehat{A}_{2M} = A_{2M-1} + R_{2M}\ A_{2M-2}, \qquad \widehat{B}_{2M} = B_{2M-1} + R_{2M}\ B_{2M-2}, \tag{120}$$

in which case the accelerated solution at a time t is given by replacing A_{2M} and B_{2M} by $\widehat{A}_{2M}$ and $\widehat{B}_{2M}$ respectively in (113).

It should be kept in mind that all the operations in equations (113) through (120) involve complex variables, and computationally intensive complex computer arithmetic must be used. Moreover, all the intermediate vectors $\vec{A}$, $\vec{B}$, $\vec{d}$, $\vec{e}$, $\vec{q}$, $\vec{a}$ and $\vec{h}$ have to be stored, which can be easily shown to require a minimum of $2N(2M_H^2 + 11M_H + 7)$ double-precision words of memory. This is very large compared to the minimal memory requirements of the Stehfest formulation.

As is shown in the second paper of this series [*Moridis*,1995], the minimum M_H for an acceptable accuracy is 5, resulting in a $N_H = 11$, which indicates that the matrix equation

(101) has to be solved a minimum of 11 times and requires $224N$ words of memory in addition to the quadrupling of the memory required for the storage of the coefficient matrix $\widehat{\mathbf{T}}$. For an accuracy comparable to that of the Stehfest method $M_H \geq 6$ and $N_H \geq 13$. The unique advantages of the DeHoog formulation is that (a) it is capable of accurately inverting very steep solution surfaces, and (b) a whole range of solutions at times t in the range $[0, T]$ can be obtained from a single set of solutions $\vec{\mathbf{X}}$, i.e. equation (101) needs not be solved for each t of interest.

The solution in the Laplace space eliminates stability and accuracy problems caused by the treatment of the time derivative in standard FD simulators, thus allowing an unlimited time-step size if the change in water density does not exceed 1.5limited to that caused by the space discretization because time is not discretized, and provides a solution inherently more accurate than the standard FD method for the same grid system. The ability to use an unlimited time-step size bounds the accumulation of roundoff error by an upper limit defined as the roundoff error accumulated after the N_S or N_H solutions. Thus, LTFD offers a stable, non-increasing roundoff error irrespective of the time of observation t_{obs} because calculations are performed at one time only by letting $\Delta t = t_{obs}$. Calculations in the standard FD method have to be performed at all the intermediate times of the discretized time domain, continuously accumulating roundoff error in the process.

9. Summary

A new numerical method, the Laplace Transform Finite Difference (LTFD) method, is extended to the solution of the solute transport problem in groundwater. The major advantage of LTFD is that it eliminates the time dependency, the need for time discretization, and the problems stemming from the treatment of the time derivatives in the nonlinear Partial Differential Equations (PDEs) of flow and transport by using Laplace transform formulations. LTFD yields solutions semi-analytical in time and numerical in space by

solving special formulations of the PDEs in the Laplace space.

The LTFD method proceeds in five steps:

1. A Laplace transform is performed on the linearized PDEs of flow and transport.
2. The transformed PDEs are approximated using a Finite Difference (FD) method.
3. The resulting system of simultaneous equations is solved in the Laplace space. The number of simultaneous equations per gridblock may vary between 1 and 6. The transformed vector of the unknown pressures and concentrations is determined in the Laplace space.
4. For very dilute solutions and time-invariant velocity distributions, there is no need for internal iterations and the process moves to Step 5. Otherwise, internal iterations are performed on the solutions of Step 3 until an acceptable convergence criterion is met.
5. The solution in time is obtained by numerically inverting the converged transformed vector of unknowns from Step 4.

Two space discretization schemes are employed in Step 2. The first uses a single-point upstream weighting, and provides only a first-order approximation. The second scheme *Saad et al.* [1990] uses an asymmetric two-point upstream weighting which provides a second- or third-order approximation. The second scheme considerably increases the size of the matrix to be solved.

Two alternative methods are used for the numerical inversion of the Laplace space solutions. The first is based on the Stehfest algorithm *Stehfest* [1970*a*], which uses real numbers for the Laplace space parameter λ_ν ($\nu = 1, \ldots, N_S$ and N_S is an even number), and requires solution of the resulting system of simultaneous equations N_S times. Linear combination of the N_S solutions returns the actual solution in time. The second method was developed by *DeHoog et al.* [1982], uses complex numbers for λ_ν ($\nu = 1, \ldots, N_H$ and N_H is an even number), and combines non-linearly the resulting N_H solutions. It requires significantly larger computer storage and execution times than the Stehfest method, but

offers the advantages that very steep solution fronts can be inverted and that predictions over a wide range of times can be obtained from a single set of matrix inversions.

If the water density changes do not exceed 1.5of the numerical treatment of the time dependency on accuracy and stability (which necessitate a large number of small time steps between successive observation times in traditional solutions) are rendered irrelevant because time is no longer a consideration. An unlimited time step size is thus possible without loss of accuracy or stability.

Acknowledgements. This work was supported by the Texas Agricultural Experiment Station under grant 6993/91, and the U.S. Department of Energy, Office of Environmental Management, Office of Technology Development, under Contract No. DE-AC03-76SF00098. The authors thank Drs. Karsten Pruess, Paul Witherspoon and Robert Zimmerman for their useful review comments.

References

Aziz, K., and A. Settari, *Petroleum Reservoir Simulation*, 476 pp., Elsevier Science, New York, 1979.

Bear, J., *Dynamics of Fluids in Porous Media*, 764 pp., American Elsevier Publishing Company, New York, 1979.

Crump, K. S., Numerical inversion of Laplace transforms using a Fourier Series approximation, *J. Assoc. Comput. Mach., 23*(1), 89-96, 1976.

DattaGupta, A., L. W. Lake, G. A. Pope, and K. Sepernoori, High-resolution monotonic schemes for reservoir fluid flow simulation, *In Situ, 15*(3), 289-317, 1991.

DeHoog, F. R., J. H. Knight, and A. N. Stokes, An improved method for numerical inversion of Laplace transforms, *SIAM J. Sci. Stat. Comput., 3*(3), 357-366, 1982.

Domenico, P. A., and V. V. Palciauskas, The volume-averaged mass-transport equation

for chemical diagenetic models, in *Developments in Water Science No. 12*, edited by W. Back and D. A. Stephenson, 427-438, Elsevier, Amsterdam, 1979.

Dorgarten, H.-W., and C.-F. Tsang, Modeling the density-driven movement of liquid wastes in deep sloping aquifers, *Groundwater, (29)*(5), 655-662, 1991.

Huyakorn, P. S., and G. F. Pinder, *Computational Methods in Subsurface Flow*, 473 pp., Academic Press, New York, 1983.

Leonard, B. P., A survey of finite differences of opinion on numerical muddling of the incomprehensible defective confusion equation, in *Proceedings, Finite Element Methods for Convection Dominated Flows*, Winter Annual Meeting of ASME, New York, Dec, 2-7, 1979.

Lantz, R. B., Quantitative evaluation of numerical diffusion (truncation error), *SPEJ Trans. AIME, 251*, 315-320, 1971.

MacDonald, J. R., Accelerated convergence, divergence, iteration, extrapolation, and curve fitting, *J. Appl. Phys., 10*, 3034-3041, 1964.

Millington, R.J., Gas diffusion in porous media, *Science, 130*, (3367),100-102, 1959.

Moridis, G. J., An implicit two-phase numerical simulator for modeling secondary water recovery by air injection, Ph.D. thesis, Dept. of Agr. Eng., Texas A&M Univ., College Station, 1987.

Moridis, G. J., The Laplace Tranform Finite Difference method for the solution of the solute transport problem in groundwater: 2. Verification and Evaluation, *Report LBL-37149*, Lawrence Berkeley Laboratory, Berkeley, Calif., 1995.

Moridis, G. J., and K. Pruess, Flow and transport simulations using T2CG1, a package of conjugate gradient solvers for the TOUGH2 family of codes, *Report LBL-36235*, Lawrence Berkeley Laboratory, Berkeley, Calif., 1995.

Moridis, G. J., and D. L. Reddell, The Laplace Transform Finite Difference (LTFD) method for groundwater simulations (Abstract), *EOS Trans. of the AGU, 71*, (17), 1990*a*.

Moridis, G. J., and D. L. Reddell, The Laplace Tranform Finite Difference (LTFD) numerical method for the simulation of solute transport in groundwater (Abstract), *EOS Trans. of the AGU, 71*, (43), 1990*b*.

Moridis, G. J., and D. L. Reddell, The Laplace Transform Finite Difference (LTFD) method for simulation of flow through porous media, *Water Resour. Res., 27*(8), 1873-1884, 1991*a*.

Moridis, G. J., and D. L. Reddell, The Laplace Transform Finite Element (LTFE) numerical method for the solution of the groundwater flow equation, (Abstract), *EOS Trans. of the AGU, 72*, (17), 1991*b*.

Moridis, G. J., and D. L. Reddell, The Laplace Transform Boundary Element (LTBE) numerical method for the solution of diffusion-type equations, in *Boundary Elements XIII*, edited by C. A. Brebbia and G. S. Gibson, pp. 83-97, Computational Mechanics Publications and Elsevier Applied Sciences, London, 1991*c*.

Moridis, G. J., and D. L. Reddell, Alternative formulations of the Laplace Transform Boundary Element (LTBE) numerical method for the solution of diffusion-type equations, in *Boundary Element Technology VII*, edited by C. A. Brebbia and M. S. Ingber, pp. 815-833, Computational Mechanics Publications and Elsevier Applied Sciences, London, 1992.

Moridis, G. J., D. A. McVay, D. L. Reddell, and T. A. Blasingame, The Laplace Transform Finite Difference (LTFD) method for the simulation of compressible fluid flow in reservoirs (SPE Paper 22888), *SPE Advanced Technology Series, 2*(2), 122-131, 1994.

Reddell, D. L., and D. K. Sunada, Numerical simulation of dispersion in groundwater aquifers, Colorado State Univ. Hydrology Paper 41, 79 pp., Colorado State Univ., Fort Collins, Colorado, 1970.

Saad, N., G. A. Pope, and K. Sepernoori, Application of higher-order methods in compositional simulation, *SPE Reservoir Engineering, 5*(4), 623-630, 1990.

Scheidegger, A. E., General theory of dispersion in porous media, *J. of Geoph. Res., (66)*(10), 3273-3278, 1961.

Stehfest, H., Algorithm 368, Numerical inversion of Laplace transforms, *J. ACM, 13*(1), 47-49, 1970*a*.

Stehfest, H., Algorithm 368, Remark on algorithm 368 [D5], Numerical inversion of Laplace transforms, *J. ACM, 13*(1), 56, 1970*b*.

Sudicky, E. A., The Laplace Tranform Galerkin technique: A time-continuous finite element theory and application to mass transport in groundwater, *Water Resour. Res., 25*(8), 1833-1846,1989.

Sudicky, E. A., The Laplace Tranform Galerkin technique for efficient time-continuous solution of solute transport in double-porosity media, *Geoderma, 46*, 209-232,1990.

Voss, C. I., *A Finite-Element Simulation Model for Saturated-Unsaturated, Fluid-Density-Dependent Ground-Water Flow with Energy Transport or Chemically-Reactive Single-Species Solute Transport*, 409 pp., U.S. Geological Survey, Reston, Virginia, 1984.

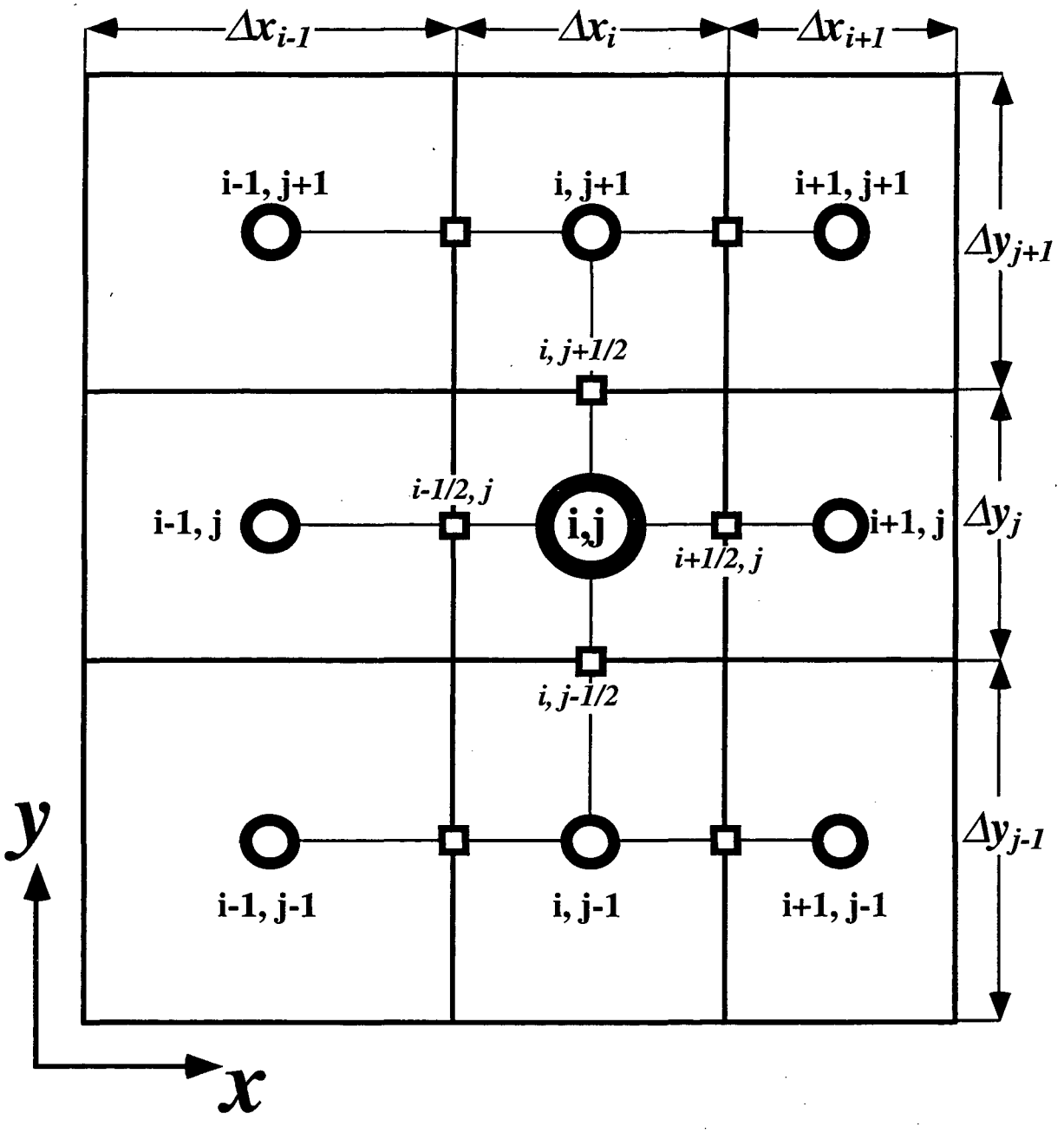

Figure 1. Discretization in a two-dimensional cartesian system (x, y).

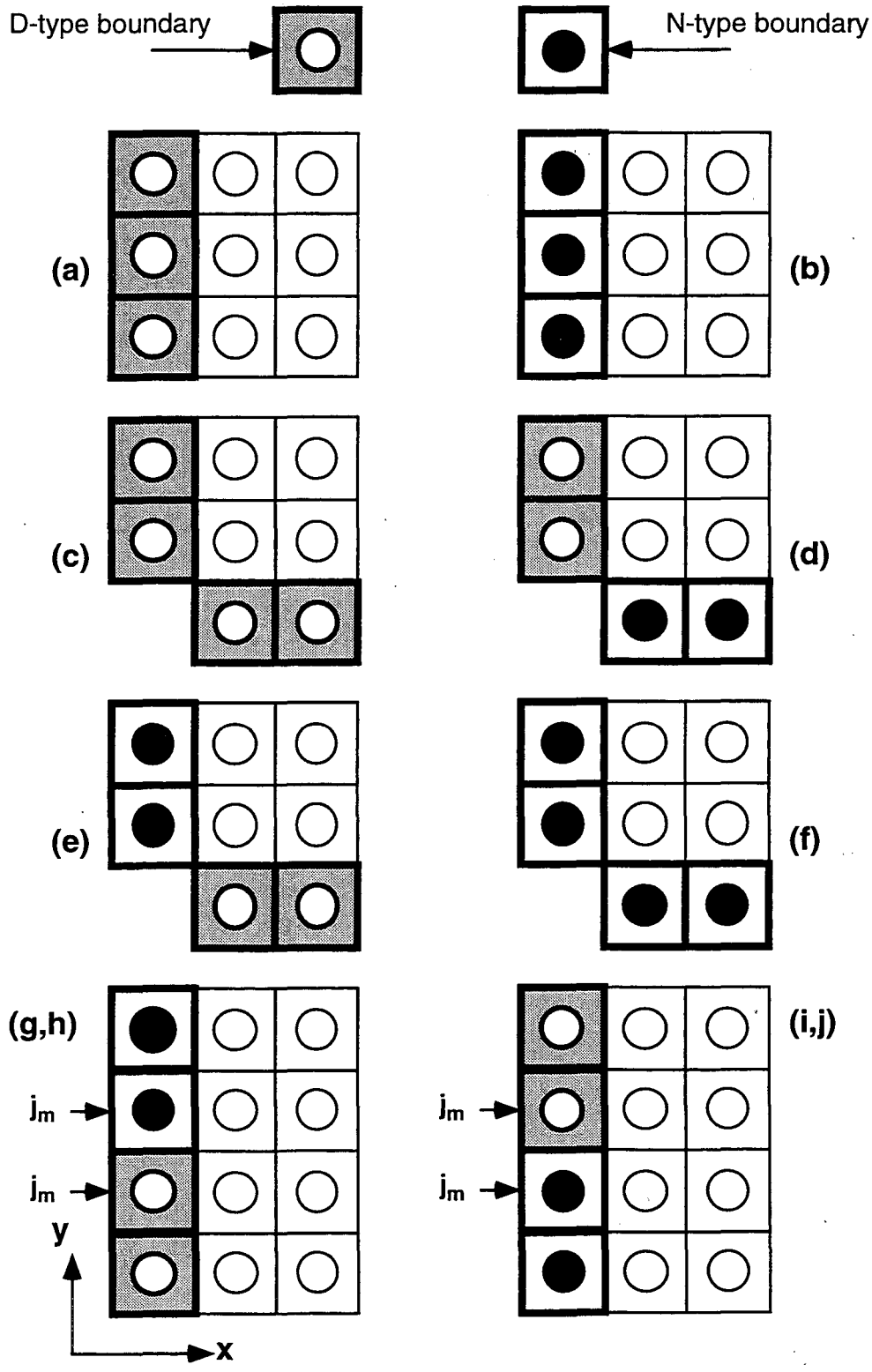

Figure 2. Possible boundary conditions in the solute transport problem.

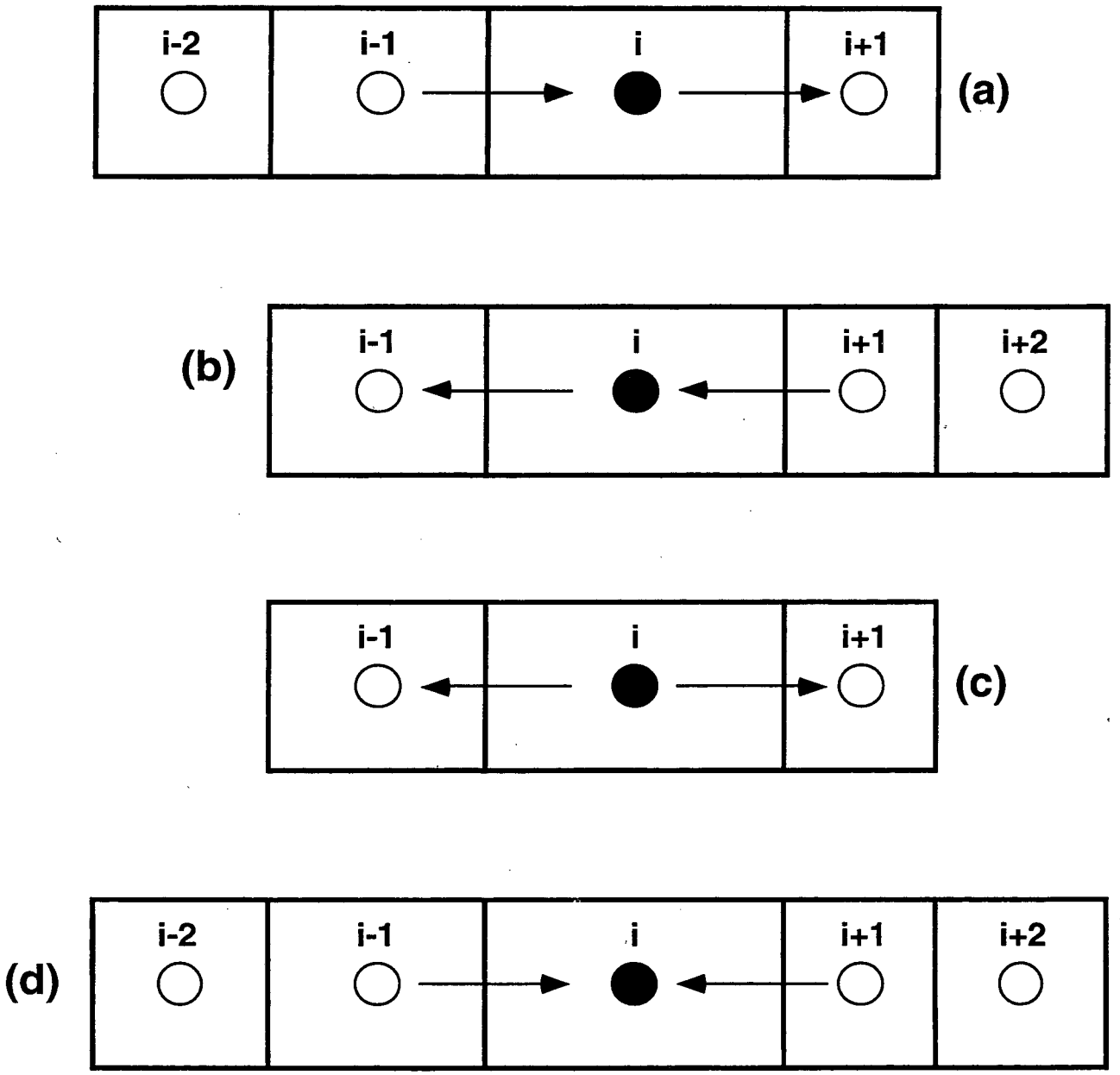

Figure 3. Application of the higher-order scheme of *Saad et al.* [1990] in the one-dimensional problem. All four possible scenarios are shown.

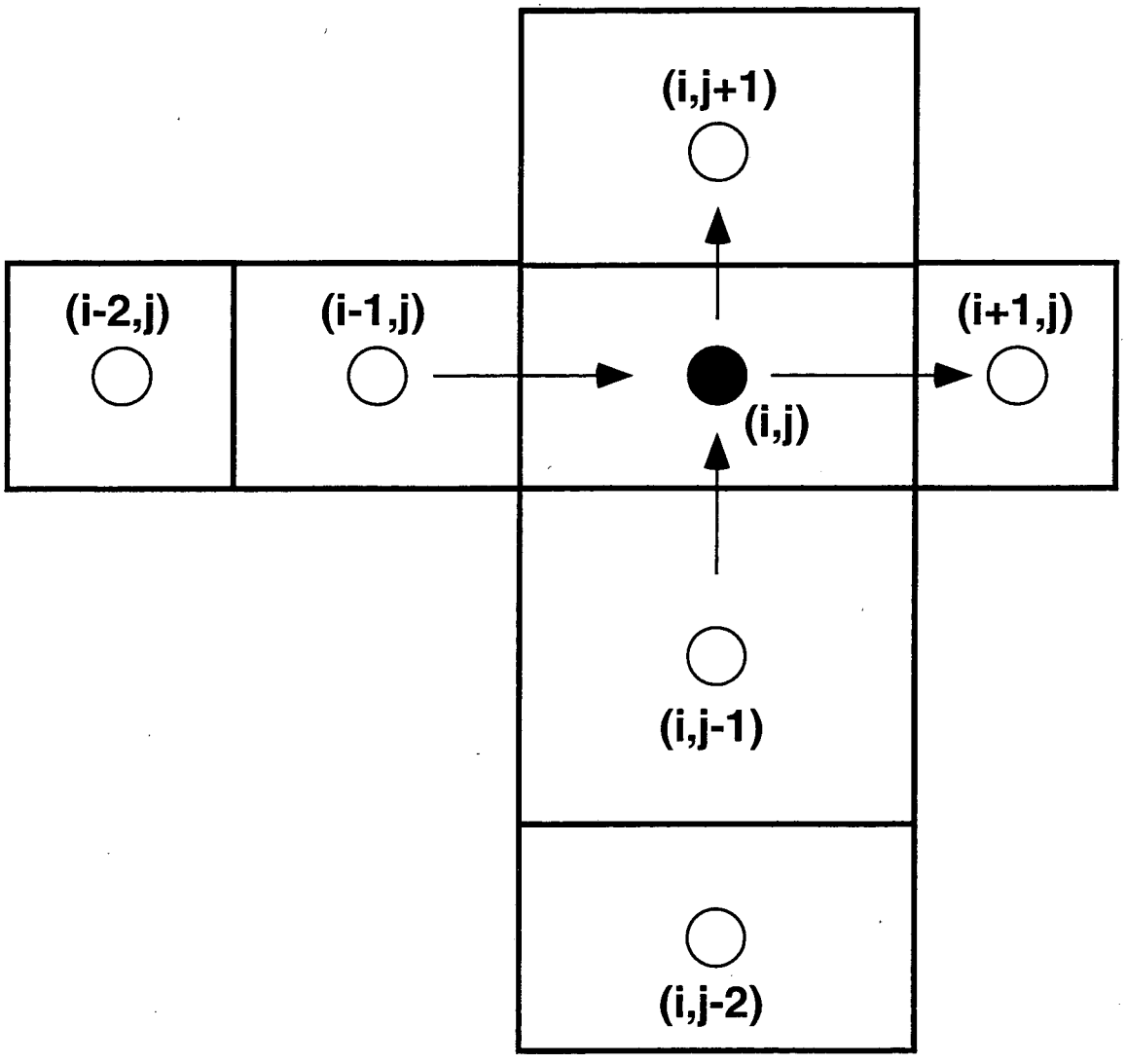

Figure 4. An example of the application of the higher-order scheme of *Saad et al.* [1990] in the two-dimensional problem.

LAWRENCE BERKELEY NATIONAL LABORATORY
UNIVERSITY OF CALIFORNIA
TECHNICAL & ELECTRONIC INFORMATION DEPARTMENT
BERKELEY, CALIFORNIA 94720